SCRATCH ELIMINATION FROM THE SURFACE OF POLYCARBONATE VISORS THROUGH AIR ATMOSPHERIC PRESSURE PLASMA JET TREATMENT

by:

Jesus Emmanuel, II F. Pimentel

Thesis submitted to the Faculty of the Physics Department
of the Ateneo de Manila University, in partial of the requirements
for the degree of Bachelor of Science in Applied Physics

2023

Advisory Committee:

Christian Lorenz S. Mahinay, Ph.D.

Giovanni M. Malapit, Ph.D.

Ivan B. Culaba, M.Sc.

This is to certify that the undergraduate thesis entitled, "**SCRATCH ELIMINATION FROM THE SURFACE OF POLYCARBONATE VISORS THROUGH AIR ATMOSPHERIC PRESSURE PLASMA JET TREATMENT**" and submitted by Jesus Emmanuel, II F. Pimentel to fulfill part of the requirements for the degree of BS Applied Physics was successfully defended and approved in December 2023.

Giovanni M. Malapit, Ph.D.
Panel Member

Ivan B. Culaba, M.Sc.
Panel Member

Christian Lorenz S. Mahinay, Ph.D.
Thesis Adviser

Joel T. Maquiling, Ph.D.
Chair, Department of Physics

ABSTRACT

Title of Document: SCRATCH ELIMINATION FROM THE SURFACE OF POLYCARBONATE VISORS THROUGH AIR ATMOSPHERIC PRESSURE PLASMA JET TREATMENT

Jesus Emmanuel, II F. Pimentel

5 – BS Applied Physics - BS Materials Science and Engineering

2023

Directed by: Christian Lorenz S. Mahinay, Ph.D.

Department of Physics

This study utilized air atmospheric pressure plasma to eliminate scratches from the surface of polycarbonate (PC) face shields. PC face shields are personal protective equipment that are generally used for construction and machine shop purposes due to their impact resistance and toughness, though they are soft and prone to scratching. The objective of the study is to improve the optical transmission properties of PC face shields by reducing or eliminating scratches from PC face shields using an atmospheric pressure plasma jet system or APPJ. The optical transmission is characterized using UV-Vis and qualitative analysis on scratch depth and number are characterized using a digital microscope. The APPJ system is composed of two tungsten electrodes encased in a borosilicate glass with a gas inlet connect to an air pump with a maximum output of 25 L/min. The tungsten electrodes are connected to a neon sign transformer capable of outputting 15 kV at 60 Hz. The data shows that the 3-second treatments lead to the most increase in transparency without any changes in focal point due to melting.

"The world is a comedy to those who think;

a tragedy to those who feel."

~ Horace Walpole

Dedication

~

To

Jacinda Therese

and

Jac Noah

~

Acknowledgements

I would like to thank the following for helping me accomplish this study:

First and foremost, to my parents, Jay and Sonia, who have raised me under the idea that I must always try my best to be a good person and have allowed me to experience love that any child should experience from their parents. Without you, I would not be here. For this, I am very grateful.

To Sir Chris, for patiently offering me guidance and help throughout my study. This thesis could not have been written without you. Thank you for accepting me as your mentee.

To Block R for being supportive to each other and for allowing each other to grow as people. I could not have asked for a better block. Thank you.

To my ride-or-die friends from high school, for being there for me especially when times got tough. You kept me sane throughout my life in Manila and seeing you brings me nothing but joy. You are my closest friends, and I am very thankful you stayed in my life.

To the labmates I have had for two and a half years, for being supportive of each other's theses and providing suggestions of their own whenever I asked for it. It was fun staying in the lab with you.

Finally, to the Plasma-Materials Interaction Laboratory in the Department of Mining, Metallurgical, and Materials Engineering in University of the Philippines - Diliman for allowing me to use their equipment to gather additional data.

Table of Contents

List of Tables

List of Figures

Chapter 1

Introduction

1.1 Background of the Study

1.1.1 Plasma and the Atmospheric-Pressure Plasma Jet

Plasma is commonly known as the fourth state of matter. It is defined as a variety of neutral substances with many free electrons and ionized molecules exhibiting collective behavior due to Coulomb forces. To characterize something as a plasma, however, there are three criteria that need to be followed [1]. These are macroscopic neutrality [2], Debye shielding, and frequency[1, 3]. To characterize a plasma, there are three different parameters that must be observed. These are particle density, the temperature of each species, and the magnetic field of the system [4].

In terms of generation, plasma is generated at atmospheric pressure by simply energizing gases. This can be done either thermally or electrically [2]. In this study, the plasma is generated electrically. This generation of plasma at atmospheric pressure saves a lot in terms of expenses due to vacuum systems being unneeded. One of the most common ways to generate and use plasma today is with the atmospheric-pressure plasma jet (APPJ). These applications are usually either with thermal plasma close to local thermal equilibrium (LTE) or with non-LTE plasma with electron temperatures much greater than the that of the heavy plasma components such as ions [5]. Atmospheric plasma is also classified in terms of their excitation mode, which are direct current (DC) discharges that are of low frequency, radio frequency (RF) discharges, and microwave discharges [2].

Applications of atmospheric plasma are widespread, ranging from medical uses to applications in materials science and engineering. For instance, cold atmospheric plasma has shown to be useful in treatment of external structures of humans, such as the skin, as well as anti-tumor effects without any detrimental effects to healthy cells

[6]. Furthermore, plasma-activated water, a potential antiseptic, can now be made using APPJs [7]. In materials science and engineering, numerous studies have been conducted to improve the properties of different materials such as wettability, surface energy [8, 9, 10, 11], and adhesion [8, 9].

1.1.2 Polycarbonate and its Properties

Polycarbonate (PC) is a thermoplastic polymer with repeat units as shown in Figure 1.1. It has two benzene rings [12] wherein these monomers are linked by carbonate (CO_3) in an $-OOCO-$ manner [13]. Among the uses for this polymer are safety helmets, lenses [12, 13], lamp housings, and in automotives [13].

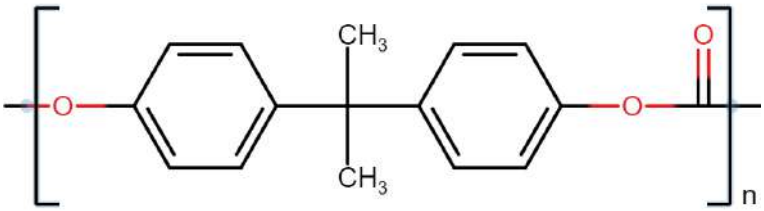

Figure 1.1: The repeat unit of PC. Made using the Marvin JS online simulator.

PC has a variety of ideal properties for everyday applications. For example, it exhibits excellent toughness up to 140°C and provides excellent electrical insulation [13]. It is transparent [12, 13] and hydrophobic while also showing great impact resistance and ductility [12]. Moreover, it has a high heat deflection temperature at ~ 130°C. It is not without its flaws, however. It has shown to be weak at resisting chemicals and ultraviolet light. Furthermore, flame retardants are a required addition to reach the highest flammability rating. In this study, our focus is on the soft nature of PC, since it also requires protective coatings to have better resistance to scratching [13].

The focus of this study is around construction-grade face shields, which typically employs PC instead of polyvinyl chloride (PVC), which is an alternative material but ultimately inferior due to its lower optical clarity and impact resistance as well as the tendency of PVC to shatter into sharp edges [14]. 3M, for example, use general purpose PC to create face shields that are used for a variety of industries such as in min-

ing, construction, and heavy infrastructure [15]. As such, the PC used for construction grade face shields are general purpose PC. Other companies may use different types of PC, though their webpages do not indicate anything.

1.2 Significance of the Study

The significance of this study hinges on the fact that PC is used for safety equipment such as safety goggles and face shields. Used in industrial and construction settings, the proneness of PC to scratching becomes a hindrance to its long-term usage. Coming up with a measure to remove these scratches could potentially increase their lifespans and reduce the need to repeatedly buy and contribute to the plastic wastes. Furthermore, this study also aims to be of guidance through the process of treating polymers using an APPJ.

1.3 Objectives of the Study

The aim of this study is to establish a foundation of further studies that investigate the capabilities of plasma to remove scratching from the surface of polymers. The more specific goals are enumerated below.

1. **Treat PC face shield using air APPJ to reduce or eliminate scratches present on its surface.** While the removal of scratches on its own cannot be objectively determined, different methods of testing shall be used in order to quantify any improvements in the PC's surface.

2. **Characterize the optical characteristics of treated PC face shield surfaces.** More specifically, this study features UVVis spectroscopy and a digital microscope to see the effect on scratch removal of the plasma on the treated PC face shields.

3. **Determine the best treatment time and type of gas while maintaining a constant nozzle to sample distance and gas flow.** This objective is related to the previous one. Treatment time is the independent variable of the study. As such,

there is an aim to determine if it has anything to do with scratch removal or with the transparency of the PC.

With these objectives in mind, indicated below are the null hypothesis H_0 and the alternative hypothesis H_1, respectively.

$\boldsymbol{H_0}$: Plasma treatment of scratched PC substrates exhibits no significant increase in transparency.

$\boldsymbol{H_1}$: Plasma treatment of scratched PC substrates exhibits a significant increase in transparency.

1.4 Scope and Limitation

This study aims to investigate the possible scratch removal properties from the surface of a PC substrate. Further studies will also be required, should another researcher want to change certain variables in this study.

Different grits of sandpapers will be used to scratch the surface of the PC substrate. Furthermore, different but specific amounts of forces will be applied to these substrates. This will be discussed further in Chapter 3.

The APPJ treatment of the PC substrates will have certain conditions. First, the distance of the nozzle from the substrate shall remain constant. The gas flow rate of the pump to be used will also remain constant. The gas that will be used in the creation of the jet is air. There will also be four given treatment times that will be used. As with the conditions of the scratching, specifics of these variables will be discussed in Chapter 3.

Furthermore, this is not a study regarding surface modifications that can be made to PC substrates. The focus of this study is to remove scratches from the surface substrates obtained from PC face shields that are available in the market. As such, this study does not include surface modifications to improve the prevention of scratches on a PC substrate.

Chapter 2

Review of Related Literature

2.1 Plasma Treatment of Polymers

Polymers are generally extremely useful at the time of writing this paper since they are flexible in terms of everyday applications [16]. Furthermore, polymerization processes are generally straightforward, as they only involve the synthesis of the monomers into large chains [12]. However, many polymers are known to have poor resistance to scratching alongside poor adhesion properties. Due to the poor resistance to scratching, certain surface modifications can be made on polymer substrates [17].

Coatings are an excellent way to modify the surface hardness of a material, but another problem comes in here because applying a good coating requires the substrate to have adhesive properties. Since polymers in general do not have these adhesiveness, applying a coating to them becomes very difficult, and surface modifications must be made in order to address this problem. The problem with this solution is that the methods of surface modification to improve adhesiveness are not budget-friendly and do not produce uniform results [8].

Due to the nature of this study, particular focus will be given to PC. Treating PC with plasma of various types is generally shown to improve wettability [8, 17], adhesion [8, 17, 18, 19], activation energy [20], and micro-hardness [21]. An increase in roughness of the PC surface has also been observed for most of these. Most of these vary in the gas used to pump the plasma, however, since some of them used Argon (Ar), Helium (He), Oxygen (O_2), and Nitrogen (N_2).

2.2 Plasma Treatment for Smoothing Polymers

Though surface roughening is observed for the treatment of PC with plasma [8, 21, 22, 23, 24], the roughening and treatment time to plasma generally have a non-linear

relation with some polymers. This factor is important since the smoothing of a surface is expected if scratches are to be removed. Even though the roughness of the surface will not be tested in this study, it is important that this is a known factor.

Three examples of polymers that exhibit smoothing after plasma treatment are poly(methyl methacrylate) (PMMA), polyvinylidene fluoride (PVDF), polyoxymethylene (POM), and polyethyl-eneterephthalate (PET). Below is a short discussion for the smoothing that happens with these polymers.

One of the tests made for plasma treatment of PMMA was its surface roughness. This was quantified using the root mean square (RMS) roughness values of a PMMA surface treated with ambient air plasma at various times with the PMMA sample located at the boundary of the plasma. Table 2.1 shows the findings of the study [9].

Table 2.1: Findings of RMS roughness values of PMMA treated with plasma based on treatment time.

Treatment Time (s)	Roughness (nm)
0	5.8
3	5.5
9	4.7
30	11.7

Different figures were also found for O_2 and N_2 plasma, but those are figures that are not of great importance here since air plasma is used in this study. What is observable here is that the increase in roughness of PMMA is not linear because its roughness initially decreases with treatment time before increasing for the 30-s treatment time [9].

A different study was conducted where changes in the surface roughness of PET was tested after plasma treatment using an APPJ. The distance of the nozzle for the treatment of the PET was 3 mm. Unfortunately, the treatment time of the PET was not provided. The results of the treatment were seen in an AFM where the RMS roughness decreases from 81 nm to 26 nm at a scale of a 30 µm × 30µm and from 16 nm to 6 nm at a 1 µm × 1 µm scale [24].

The same study analyzed the RMS roughness for PVDF as well. This time, the nozzle was placed 10 mm from the substrate. The changes in the RMS roughness of the PVDF after plasma treatment was not as pronounced as what was seen in PET, but is worth mentioning regardless. At a 10 µm × 10 µm scale, the change in the RMS roughness was from 10 nm to 8 nm [24].

For both of these studies, it was determined that the main contributor to the changes in the surface topology of the polymer was the thermal effects of the exposure of the polymer to plasma. This is because the plasma jet can have very high temperatures ranging from 600 K to 1200 K [24].

Finally, another study also found that plasma treatment of PMMA and POM resulted in a reduced static and kinetic coefficient of friction. It was found also that the usage of N_2 plasma is generally best for this sort of application due to its chemically reactive nature creating bonds with the surface molecules of PMMA and POM creating new functional groups with the creation of C−O, C=O, C−N, and C=N bonds [23]. For PC substrates, no such new bonds were observed from N_2 plasma treatment, with only the intensifying of the C−O and C=O bonds exhibited [21].

2.3 Ultraviolet-Visible Light Spectroscopy

Ultraviolet-visible light spectroscopy (UV-Vis) refers to a variety of techniques that use light transmission as a function of wavelength to give an experimenter information about the "electronic transitions" occurring in a material [25].

There are a variety of methods used to make spectroscopic measurements with UV-Vis. The four main methods are transmission, diffuse, reflectance, and absorption spectroscopy [25]. The transmission UV-Vis spectroscopy is of particular interest in this case.

The transmission UV-Vis is a method of testing the degree of transparency of a material based on some baseline measurement where 100% transmission is observed. This baseline is determined by using a perfectly transparent material where the intensity of the incident light ray used (I_0) is equal to the transmitted intensity (I). It is required

that the sample to be used for this testing is not completely opaque [25].

Chapter 3

Methodology

3.1 The APPJ Setup

The APPJ to used in this study consists of a variety of parts. The plasma is generated using two Tungsten (W) electrodes about 1 cm apart, both connected to a circuit with a transformer that provides a voltage of 10 kV. These electrodes are made stationary inside a borosilicate apparatus using corks. The apparatus used for this study was purchased from B.E. Scientific and consists of two gas inlets at its top, two inlets for the electrodes, and one outlet nozzle about 2.5 mm in diameter. One gas inlet is covered for this study due to the absence of a splitter. The other gas inlet was connected to an electric air pump by rubber tubes. The air pump emits gas into the inlet at a flow rate of 25 L/min. The gas being pumped comes out of the nozzle bringing with it energized species therefore creating a plasma jet at atmospheric pressure. Figure 3.1 shows a schematic diagram of the setup circuit.

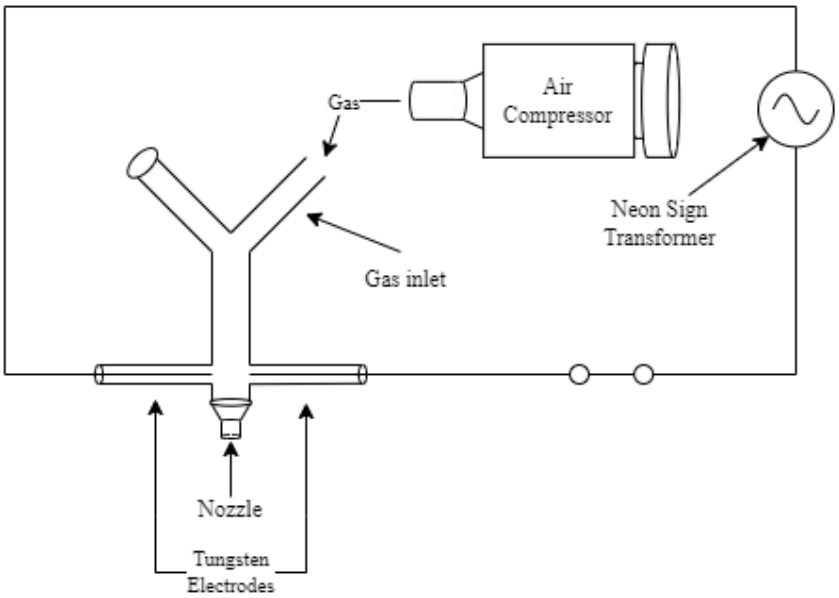

Figure 3.1: Schematic diagram of the setup circuit.

The glass is mounted on an aluminum clamp which is in turn mounted on an aluminum stand. This clamp is adjusted along an up-and-down direction in such a way that the substrate is 5 mm below the nozzle. This nozzle distance measurement is directly taken from the study conducted by Zafra [8]. Figure 3.2 shows a photo of the actual setup.

Figure 3.2: Actual photo of the APPJ.

3.2 Obtaining and Cleaning the PC Substrate

The PC substrates were purchased online from Tolsen Tools and More. The PC substrates were derived from an industrial grade face shield. These were cut into rectangles with dimensions 1in $\times$ 1in. The substrate used was found to be 1 mm thick using a digital caliper.

The PC Substrates were then soaked in distilled water with liquid soap. Afterwards, they were dabbed with Kimwipes to dry the surface of the PC. These were then wiped with 70% alcohol. For storage, the PC substrates were stored wrapped in Kimwipes and in a sealed container.

3.3 Scratching the PC Substrates

The PC substrates were then scratched using calibrating weights of various mass and different grits of sandpaper. The weights were obtained from the physics laboratory of Ateneo de Manila University located in the SEC-C building. The weights obtained are detailed in Table 3.1.

Table 3.1: The quantity and mass of each calibrating weight.

Quantity	Mass (g)
3	500
8	100
5	50

The sandpaper used was obtained from the online market and had grits of 2000, 1500, and 1000. The weight was placed above the smooth part of the sandpaper while its abrasive part was in contact with the substrate. The was then dragged across the substrate along one direction. Only one pass was made with this setup to scratch the substrate to simplify the process. Figure 3.3 shows the schematic diagram of this process.

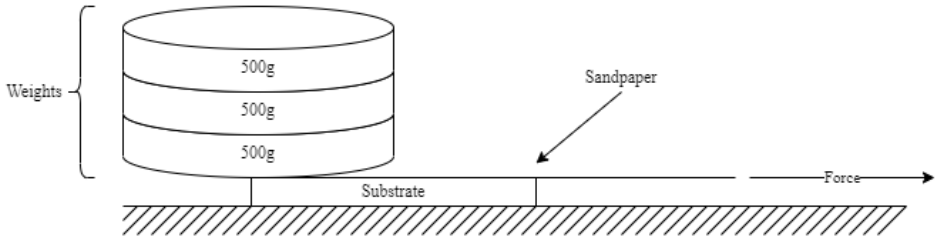

Figure 3.3: Schematic diagram of the scratching setup.

The substrates were scratched with the masses as shown in Table 3.1. The scratching was done until the lightest scratches became visible. The "lightest visible" scratches are subjective in nature, but these were nonetheless tested with UV-Vis transmission spectroscopy. This part of the scratching was done using the 2000 grit sandpaper. After finding a specific amount of weight that allows for such condition, these same weights were used for the 1500- and 1000-grit sandpapers to scratch other substrates.

However, there are some substrates that were scratched with them being attached to the weights and being dragged across the sandpaper instead. From a macroscopic standpoint, the only visible difference this made was that the scratching on the substrate became much more even. It was observed that for some substrates, the initial setup produced scratches that were specific to the center of the substrate, whereas the latter setup allows for scratching throughout the entirety of the substrate.

3.4 Plasma Treatment of the PC Substrate

The PC substrates were placed 5 mm under the nozzle of the APPJ. The treatment times for these substrates were 3 seconds, 5 seconds, 7 seconds, and 9 seconds. These times were recorded using a digital timer.

3.5 Macroscopic Analysis of the PC Substrate

Due to the nature of the usage of this kind of substrate in face shields, the eye test is important. As such, a macroscopic analysis of any changes to the PC Substrate were duly noted of. Any changes that can be seen at a macroscopic level such as image distortions, non-quantitative increase in optical clarity, or melting on the surface will affect the overall feasibility of using an air APPJ to remove the scratches from the surface of these PC substrates.

For the purpose of this study, a USB camera capable of up to 1600× zoom was also employed. The images were then taken using the Hi-view application. Each of these images were then taken. The reason behind this is to see from a small level the qualitative differences in opacity of each of the substrates. Therefore, the USB camera is used essentially as a method of macroscopic analysis of the substrates.

The photos taken were of the substrates. Due to the transparent nature of PC, it is required that the background used also be uniform. To be able to clearly see the scratches, which are white in color, the substrates were placed on top of black electrical tape on a table. This can be visualized in Figure 3.4.

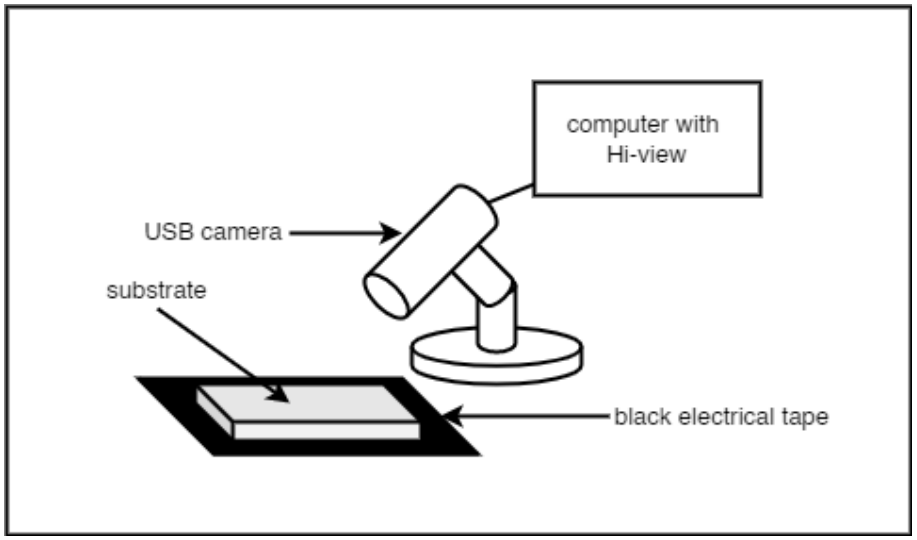

Figure 3.4: Schematic diagram of the USB camera setup.

3.6 Spectroscopy for the PC Substrate

Transmission UV-Vis spectroscopy was done to test the scratch removal on the PC Substrates. An incident light of intensity I_0 was shone on the substrate with a spectrometer behind the substrate testing the transmitted intensity of the light I_t. These intensities are then compared to each other.

The UV-Vis spectrometer was calibrated by finding the light and dark transmission spectra. This is the standard method of calibration recommended by the user manual of the manufacturer. These calibrations were done in succession before every use, that is, each time the spectrometer is turned on or has remained idle for more than 30 minutes.

To begin, an initial UV-Vis test for the clean PC substrate was done to establish a baseline I_0 for each sample. Another test was done after scratching to determine the reduction of I_t relative to I_0. To end, the treated PC substrate was tested again for a new I_t.

The relative transmittance is calculated using Equation (3.1). In order to not be confused by the symbols later on, the following notation will be used. The relative transmittance will be represented as I_{rel}. I_0 will always refer to the baseline transmittance of the PC substrate. The variable I_s will refer to the transmittance of the scratched PC

substrate. Finally, I_t will refer to the transmittance of the substrates treated with plasma. For now, however, I_t will be used to denote any non-baseline transmittance.

$$I_{\text{rel}} = \frac{I_t}{I_0} \tag{3.1}$$

The relative transmittance is then recorded into a table. From this table, a transmittance vs. wavelength curve is generated.

The UV-Vis Transmittance spectroscopy was done using a Theta Metrisis FR-Pro provided by the Department of Science and Technology to the Vacuum Coating and Plasma Physics Laboratory of Ateneo de Manila University. The parameters were set to transmittance spectroscopy with the % option on. The transmittance testing considered a minimum of three different layers. These were set to the following parameters:

1. Air until boundary, that is, the air is set at a thickness or distance a new refractive index is detected.
2. PC (Polycarbonate) with thickness 1 mm.
3. Air until infinity, which is essentially a setting that sets the final medium through which the light travels to air until it reaches the detector that measures the intensity of the transmitted light.

Figure 3.5 shows the complete setup of the UV-Vis spectrometer in the Vacuum Coating and Plasma Physics Laboratory of Ateneo de Manila University.

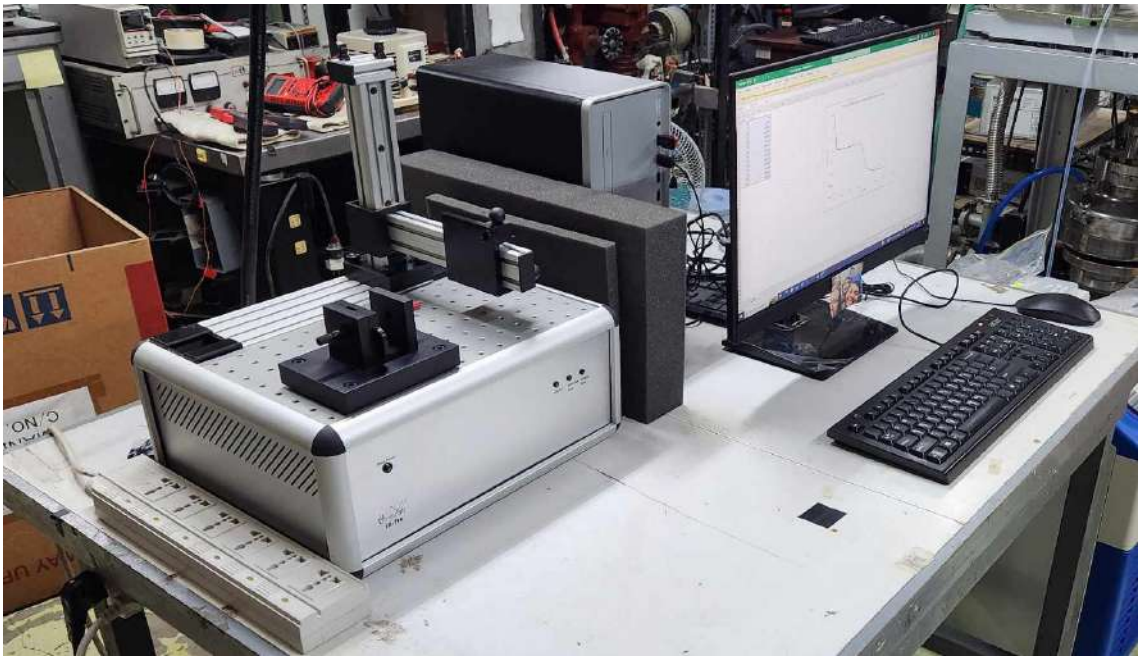

Figure 3.5: Actual photo of the UV-Vis setup.

With the generated tables and curves, the software Origin was used to find the area under each of the spectra [26].

3.7 Statistical Analysis

The first part of the statistical analysis focuses on the relation between the treatment time and the resulting transparent area of the substrates scratched. This relation was interpreted by creating a scatter plot of the areas of the transparent parts using Microsoft Excel. Using the same application, the equation of the trendline and the R^2 values were provided. Finding the R values was done by simply calculating the square root of R^2 to determine the strength and considering the slope of the trendline to determine the type of relationship (positive or negative). The strength of the relationship based on the R value was done based on Table 3.2 [27].

After this, the relative transmittance was plotted against the treatment time. Different regression tests were then done to determine the best description of the relation between the transmittance and treatment time. Linear, logarithmic, power, and exponential regressions will all be used. The "best" description will be determined using the R^2 value for each trendline generated.

Table 3.2: R values and strength of correlation.

R value	Level of Correlation
0.00-0.30 (0.00-−0.30)	Negligible correlation
0.30-0.50 (−0.30-−0.50)	Low positive (negative) correlation
0.50-0.70 (−0.50-−0.70)	Moderate positive (negative) correlation
0.70-0.90 (−0.70-−0.90)	High positive (negative) correlation
0.90-1.00 (−0.90-−1.00)	Very high positive (negative) correlation

The selection of a trendline was done based on the wavelength ranges of specific colors specified by Table 3.3 [28].

Table 3.3: Wavelength ranges for each color in the visible spectrum.

Color	Wavelength Range (nm)
Violet	380-450
Blue	450-495
Green	495-570
Yellow	570-590
Orange	590-620
Red	620-750

Table 3.3 specifies the boundary wavelength in which a color can be visible. This study takes the entire range of wavelengths into consideration. As such, to find out how well the relative transmittance is improved across the entire spectrum, the area under the spectrum from $\lambda = 250.209$ nm to 899.891 nm will be taken using Origin. The entire spectrum shown in the figures are taken into consideration to account for the transmittance of UV and IR light, especially with the latter displaying detrimental effects to humans [29]. The areas under each of these curves was then plotted in relation to the treatment time to find the optimal treatment time. Furthermore, the areas under the curve of each spectrum was compared to the spectrum of the pristine sample by taking the difference in area of the pristine spectrum and the treated spectrum.

Chapter 4

Results and Discussion

4.1 Scratching of PC Substrates

The PC Substrates were initially scratches using a 2000-grit sandpaper. Figure 4.1 shows the results of the scratching. In the figure, the weight applied on the changed in an increasing order with the weights 300g, 500g, 1000g, and 1500g.

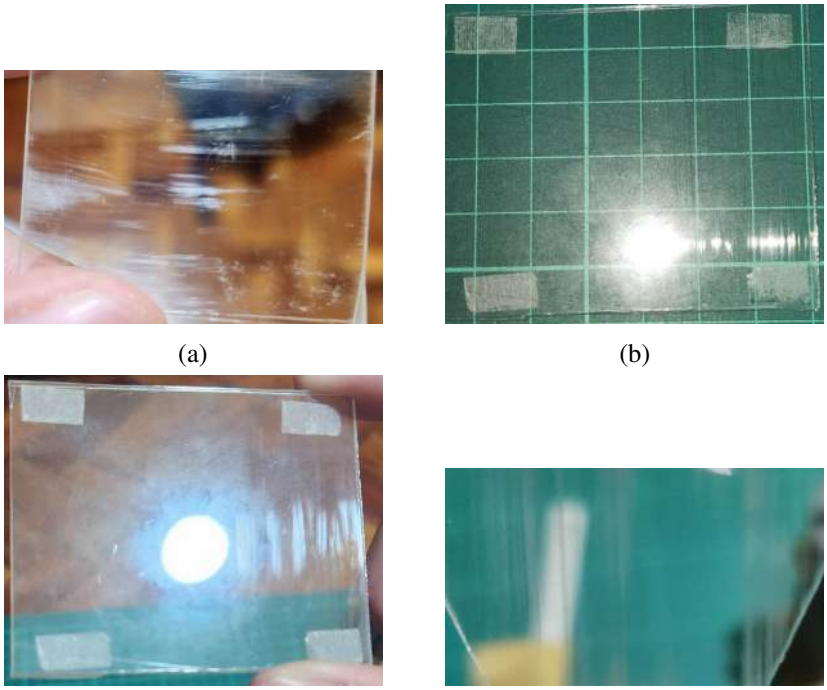

(a) (b)

(c) (d)

Figure 4.1: Resulting scratches of the PC Substrates with 2000-grit sandpaper using (a) 300g/2.94N, (b) 500g/4.9N, (c) 1000g/9.8N, and (d) 1500g/14.7N of weight.

In Figure 4.1a, scratching is only visible from a certain angle under a commercial-grade LED. The same can be said for Figure 4.1b and Figure 4.1c, though a noticeable trend in visibility of the scratches is increasing. Finally, in Figure 4.1d, the scratches were visible even without light. This means that there is some degree of opacity as a result of scratching the PC substrate with 1500g of calibrating weights – or 14.7N of force – with a 2000-grit substrate. The 1500-g set of calibrating weights was used for

the rest of the scratching of the substrates for the 1000- and 1500-grit sandpapers, as well.

4.2 Images from USB Camera

The images retrieved from Hi-view and the USB camera are discussed in this section. First, the unscratched version of the substrate will be inspected. This will then be followed by the scratched versions of the substrates subjected to the different grits of sandpaper used. To end, the photomicrographs of the treated samples will be shown. All of these photomicrographs have scale bars at the bottom-right part of the images that indicate a length of 5 mm. The photo of the photomicrograph used for the calibration of the images will be shown in A.1.

The photomicrographs of a substrate scratched with 1000-, 1500-, and 2000-grit sandpaper are presented. These are shown in Figures 4.2a, 4.2b, and 4.2c, respectively.

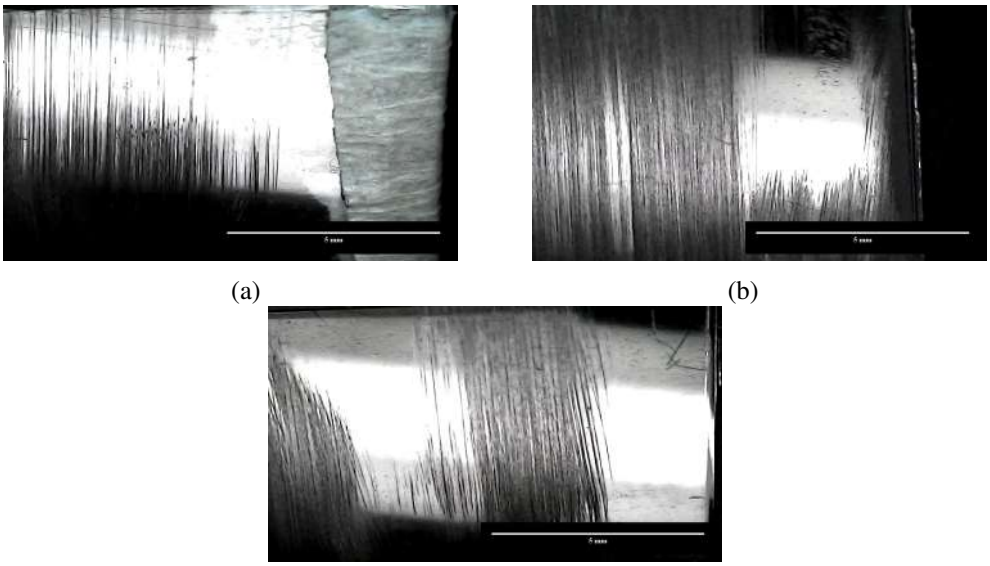

(a) (b)

(c)

Figure 4.2: Photomicrographs of the PC scratched with (a) 1000-, (b) 1500-, and (c) 2000-grit sandpaper.

Because the details of the electrical tape background are not visible compared to with Figure 4.2, we can say that there is a significant decrease in the transparency the substrate.

Figure 4.3 shows us the photomicrographs of the substrates scratched with a 1000-grit sandpaper and treated with the APPJ for 3 seconds.

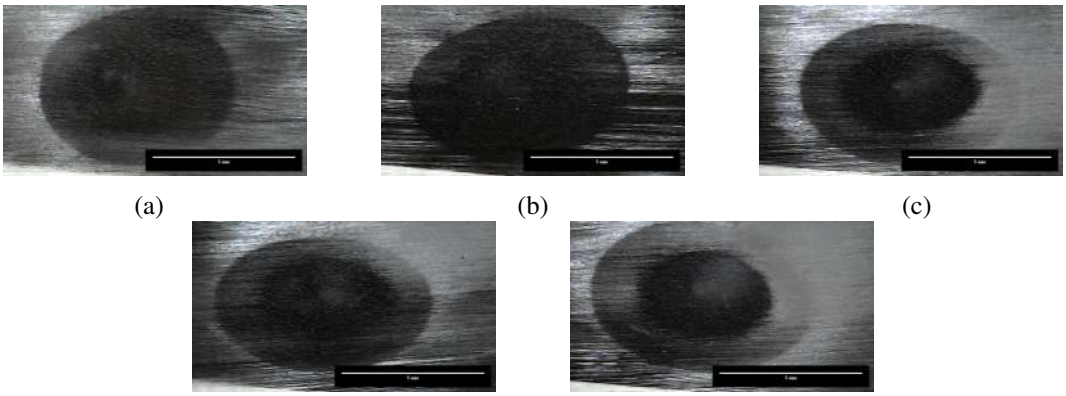

(a) (b) (c)

(d) (e)

Figure 4.3: Substrates scratched with 1000-grit sandpaper and treated for 3 seconds where (a) to (e) are Trials 1 to 5, respectively.

Figure 4.3 shows that there is a significant increase in the transparency of each substrate's center compared to the photo shown in Figure 4.2a. This increase in transparency is in the shape of an ellipse. For Figures 4.3a and 4.3b, the clarity can be seen for the entirety of the ellipse. On the other hand, for Figures 4.3c, 4.3d, and 4.3e, the clarity increases in the center with the clarity decreasing in what appears to be a stepwise manner going out from the center.

Figure 4.4 shows the resulting photomicrographs for the substrates that underwent a 3-second treatment with the APPJ. More specifically, these were the substrates scratched with 1500 grit sandpaper.

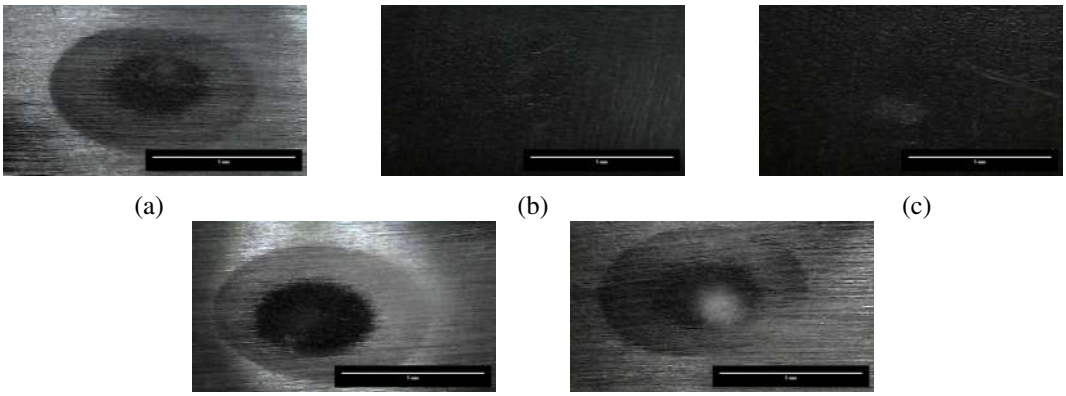

(a) (b) (c)

(d) (e)

Figure 4.4: Substrates scratched with 1500-grit sandpaper and treated for 3 seconds where (a) to (e) are Trials 1 to 5, respectively.

For Figures 4.4a, 4.4d, and 4.4e that essentially the same results can be found as in 4.3. These same results are not as visible in Figures 4.4b and 4.4c because the scratches themselves are not visible. This can be explained by the fact that the scratching for these substrates was done using the method in Figure 3.3. This resulted in uneven scratching and due to the area of the treated part, the scratching already disappeared.

The final set of photomicrographs from the USB Camera for the 3-second treatments are found in Figure 4.5. The substrates in this case were scratched using 2000-grit sandpaper.

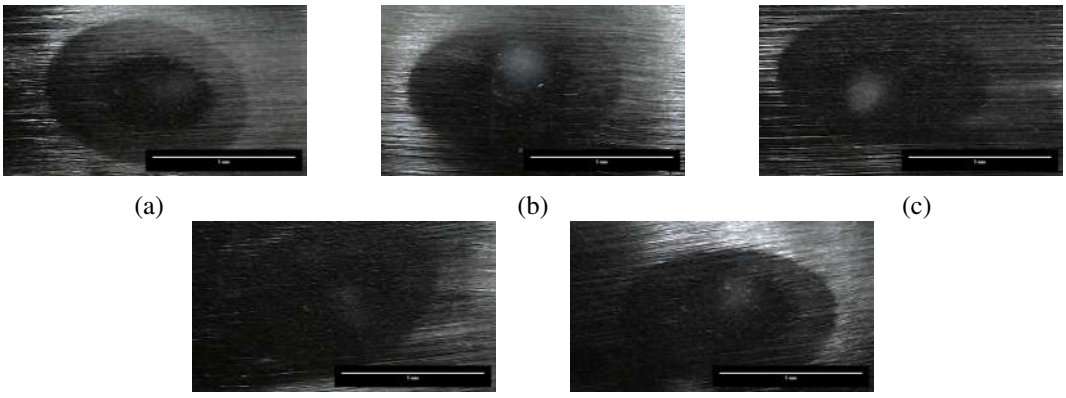

(a) (b) (c)

(d) (e)

Figure 4.5: Substrates scratched with 2000-grit sandpaper and treated for 3 seconds where (a) to (e) are Trials 1 to 5, respectively.

The results of the treatment are consistent with the results found in Figures 4.3 and 4.4. However, it can be noticed that for this treatment, white spots begin forming around the center of where the clear areas are. This can be explained by the increase in roughness of the substrate after 3 seconds. Table 2.1 shows that the smoothing effect of plasma on rough substrates is non-linear, that is, the resulting surface roughness is not directly proportional to the treatment time [9]. From this, it can also be said that the smoothing effect of plasma is also related to the roughness of the surface itself. With this in mind, we can say that because the roughness resulting from scratching a surface 2000-grit sandpaper is less than the roughness if the surface were scratched by 1000- or 1500-grit sandpaper, the roughness begins to increase again for the PC substrates after 3 seconds.

The stepwise decrease in transparency going away from the center is illustrated in Figure 4.6.

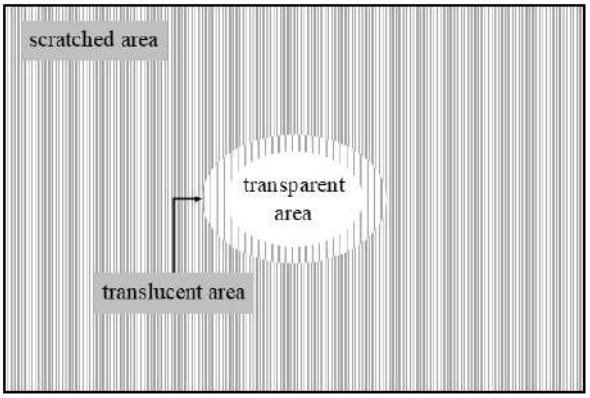

Figure 4.6: General diagram of treated substrate.

In Figure 4.6, areas of high transparency are close to the center and labelled, appropriately, as the transparent area. On the other hand, the area of reduced transparency relative to the rest of the scratched areas but with lower transparency compared to the transparent area will be labelled as translucent.

Because the resulting treatments show treated areas that are elliptical in nature, it may be useful to find the lengths of its major and minor axes. Table 4.1 shows these data. "N/A" was used for any of the samples wherein no translucent area was found. In the table, the length of the major axis is labelled as "Ma. Axis" while the length of the minor axis is labelled as "Mi. Axis". As with how ellipses are described mathematically, the major axis is the line along the long part of the ellipse while the minor axis is line along the shorter part of the ellipse. Referring to Figure 4.6, the major axis is a horizontal line passing the middle of the substrate, while the minor axis is a vertical line passing the center of the substrate.

Table 4.1: Length of minor and major axes of the area treated for 3 seconds.

Grit	Trial	Transparent		Translucent	
		Ma. Axis (mm)	Mi. Axis (mm)	Ma. Axis (mm)	Mi. Axis (mm)
1000	1	6.800	5.236	N/A	N/A
	2	7.730	5.065	N/A	N/A
	3	4.689	2.970	7.656	4.944
	4	4.535	3.109	7.625	4.690
	5	4.698	3.113	7.878	5.321
1500	1	3.236	2.090	7.281	4.421
	2	2.563	3.251	N/A	N/A
	3	3.365	1.824	N/A	N/A
	4	4.025	2.601	7.633	4.852
	5	3.576	2.014	7.237	4.538
2000	1	3.875	2.679	7.132	5.032
	2	7.465	4.006	N/A	N/A
	3	7.297	4.757	N/A	N/A
	4	6.220	4.897	N/A	N/A
	5	3.908	2.545	7.389	4.659

From the data in Table 4.1, the average dimensions of the ellipse at which the APPJ treatment is effective can be determined. There will be two cases involved. The first criteria is the average area of the transparent part of the substrate after treatment which will be called the "effective area". The second case involves the average area wherein the scratches were reduced which we will call the "treated area". The difference between these two parameters is that treated dimensions also consider the translucent areas. The data for this is shown in Table 4.2.

Table 4.2: Effective and treated dimensions of the substrates treated for 3 seconds.

	Ma. Axis (mm)	Mi. Axis (mm)	Area (mm^2)
Effective Area	4.932	3.344	12.953
Treated Area	6.751	4.500	23.859

Table 4.2 shows that transparency is achieved after 3 seconds of treatment for 12.953 mm^2 while scratches are generally reduced within an elliptical area of 23.859 mm^2. This is a small area especially compared to the 400 mm^2 area of the entire substrate.

Figure 4.7 shows the photomicrographs of the substrates scratched with 1000-grit sandpaper and then treated for 5 seconds.

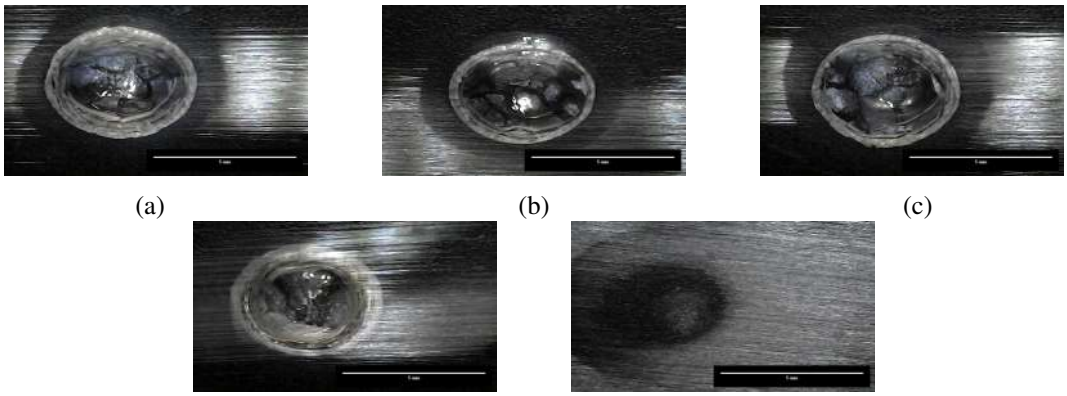

Figure 4.7: Substrates scratched with 1000-grit sandpaper and treated for 5 seconds where (a) to (e) are Trials 1 to 5, respectively.

Figures 4.7a, 4.7b, 4.7c, and 4.7d exhibit a deformation forming in the proximity of where the nozzle was located. This deformation is likely a result of the melting of PC due to high temperatures. The last treatment, on the other hand, looks similar to the results found in Figure 4.5 and exhibits no deformation. A possible explanation for this is that the treatment for Figure 4.7e was done on a different day, when the APPJ was not active for a longer amount of time. This inconsistency in the results does not apply for the 3-second treatments because this result is an outlier whereas the absence of deformations in the 3-second treatments is consistent.

Figure 4.8 shows the resulting photomicrographs of the substrates scratched with 1500-grit sandpaper and then treated for 5 seconds.

In all five photomicrographs, the deformations seen in Figure 4.7 are also seen. However, there are two observations that are specific to 4.8c and 4.8d. For 4.8c, there are visible black marks along the skirts of the melted area's right-hand side. On the other hand, Figure 4.8d shows a reflection of orange light close to the center of the melted area.

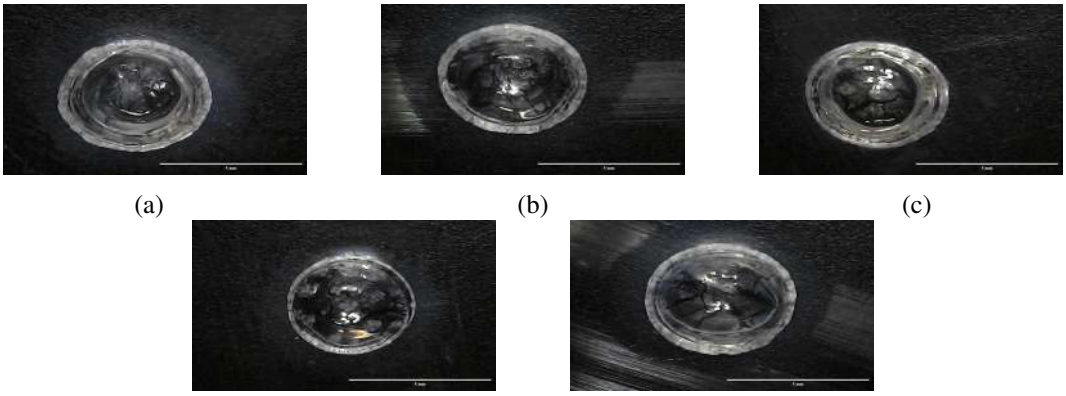

(a) (b) (c)

(d) (e)

Figure 4.8: Substrates scratched with 1500-grit sandpaper and treated for 5 seconds where (a) to (e) are Trials 1 to 5, respectively.

Figure 4.9 shows the photomicrographs for the substrates scratched with a 2000-grit sandpaper then treated for 5 seconds.

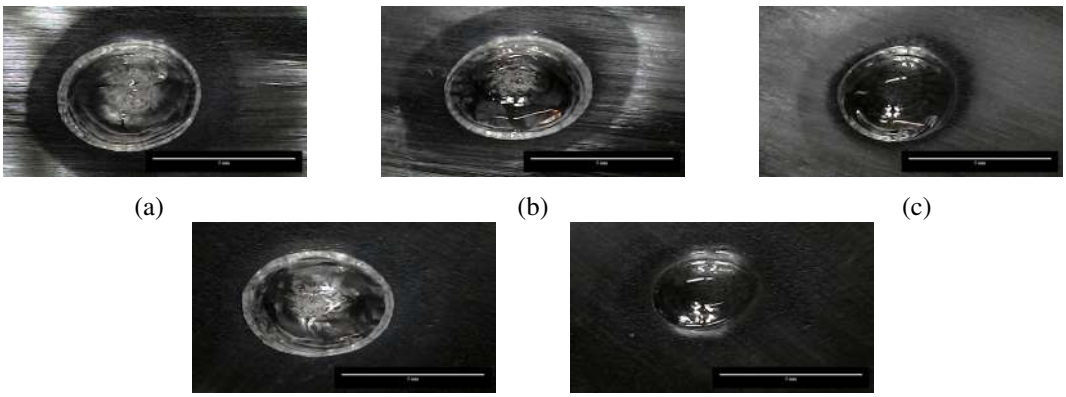

(a) (b) (c)

(d) (e)

Figure 4.9: Substrates scratched with 2000-grit sandpaper and treated for 5 seconds where (a) to (e) are Trials 1 to 5, respectively.

The melting of the PC remains consistent in this case. There are also some notable observations for specific substrates. Figure 4.9b displayed some bubbling in the center. This same photomicrograph, as well as Figure 4.9d, displayed reflectance of orange light along the outskirts of the melted area. Finally, an elliptical area was observed to have a transparency without melting in Figure 4.9c. This clear area can be seen to have a major axis length of 5.098 mm and a minor axis length of 3.906 mm.

Table 4.3 shows almost the same data as Table 4.1. The main difference in this case is that we have observed melting in the substrates treated for 5 seconds. As such, the initially labeled effective area is now referred to as the melted area.

Table 4.3: Length of the minor and major axes of the area treated for 5 seconds.

Grit	Trial	Melted		Translucent	
		Ma. Axis (mm)	Mi. Axis (mm)	Ma. Axis (mm)	Mi. Axis (mm)
1000	1	5.333	3.933	7.278	4.756
	2	5.133	3.489	7.056	N/A
	3	5.238	3.969	7.341	N/A
	4	4.392	3.092	N/A	N/A
	5	4.447	2.805	N/A	N/A
1500	1	5.456	3.933	N/A	N/A
	2	5.274	3.852	8.089	4.256
	3	5.033	3.727	N/A	N/A
	4	4.518	3.437	N/A	N/A
	5	5.368	3.845	N/A	N/A
2000	1	5.069	3.873	7.530	5.878
	2	5.167	3.700	8.611	5.691
	3	4.125	3.287	6.882	5.550
	4	5.367	3.744	N/A	N/A
	5	3.690	2.469	6.796	3.871

**"N/A" measurements when scratches are not wide enough to make an accurate measurement.*

The average dimensions and area of the melted ellipses can be found in Table 4.4 alongside the treated dimensions and area.

Table 4.4: Melted and treated dimensions of the substrates treated for 5 seconds.

	Ma. Axis (mm)	Mi. Axis (mm)	Area (mm^2)
Melted Area	4.907	3.544	13.658
Treated Area	6.278	4.136	20.393

In summary for this part of this section, elliptical deformations form by melting after 5 seconds of treatment. While there is an increase in the transparency of the substrate after this treatment, this also leads to the formation of deformations on the surface of the material and a change in its optical focal point. This change in focal point results in the blurring and distortion of images which is detrimental for applications such as with face shields where optical transparency is important. Furthermore, the area of treatment is generally an ellipse with an average major axis length of 6.278 mm and a minor axis length of 4.136 mm, which gives a resulting area of 20.393 mm^2, which is small especially when compared to a 400-mm^2 substrate.

Figure 4.10 shows the resulting photographs of the 7-second treatments for the substrates scratched with a 1000-grit substrate.

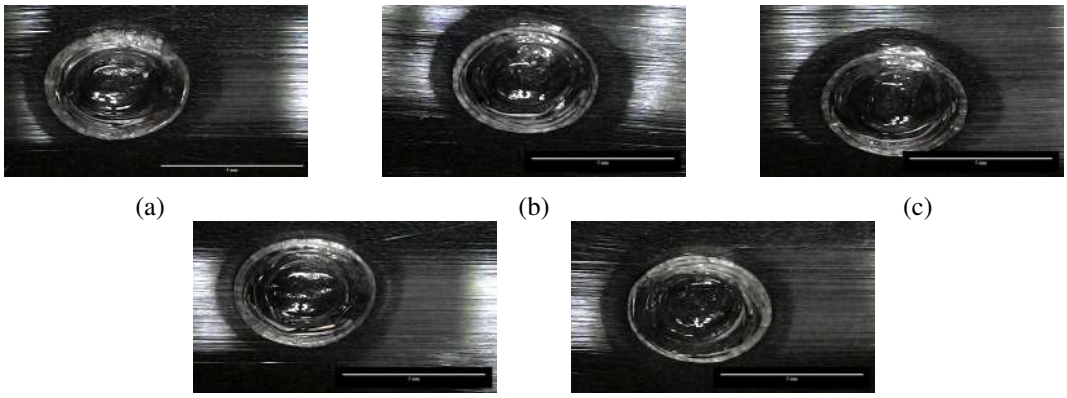

Figure 4.10: Substrates scratched with 1000-grit sandpaper and treated for 7 seconds where (a) to (e) are Trials 1 to 5, respectively.

The same deformation in this figure can be observed as in Figures 4.7, 4.8, and 4.9. However, the photos show a much clearer view of the electrical tape than the substrates treated for 5 seconds. Furthermore, it can be observed that for all these photomicrographs that there is a transparent area around the melted area. However, this area is only measurable for Figures 4.10b and 4.10c. For Figure 4.10b, this transparent area has a major axis length of 5.681 mm and a minor axis length of 4.759 mm. On the other hand, for Figure 4.10c, this transparent area has a major axis length of 6.567 mm and a minor axis length of 4.768 mm.

Figure 4.11 shows the photomicrographs of the substrates scratched with 1500-

grit sandpaper and then treated for 7 seconds.

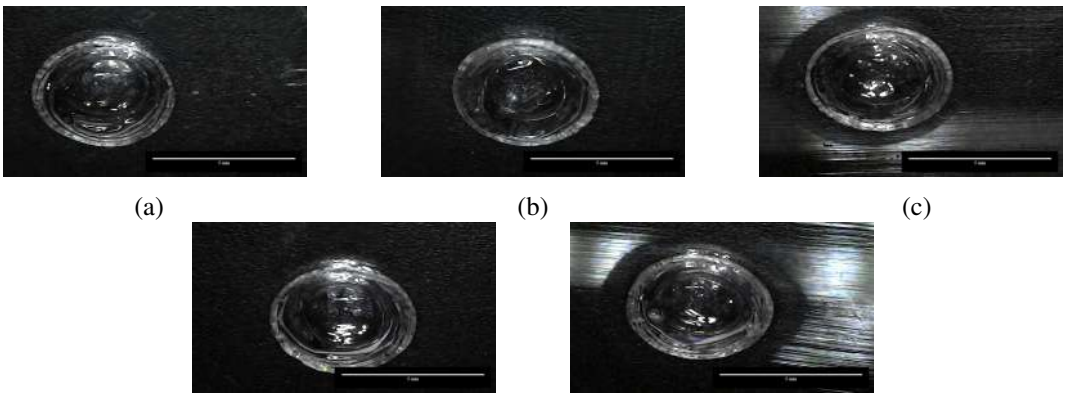

(a) (b) (c)

(d) (e)

Figure 4.11: Substrates scratched with 1500-grit sandpaper and treated for 7 seconds where (a) to (e) are Trials 1 to 5, respectively.

In Figure 4.11d, a yellow-green speck can be observed at the edge of the melted area. This is likely reflected light. The photomicrographs provided here are similar in nature to those found in Figure 4.10. However, the melted area for Figure 4.11 is noticeably less transparent compared to that of the ones scratched with 1000-grit sandpaper.

Figure 4.12 shows the resulting photomicrographs of the substrates treated for 7 seconds after being scratched with a 2000-grit sandpaper.

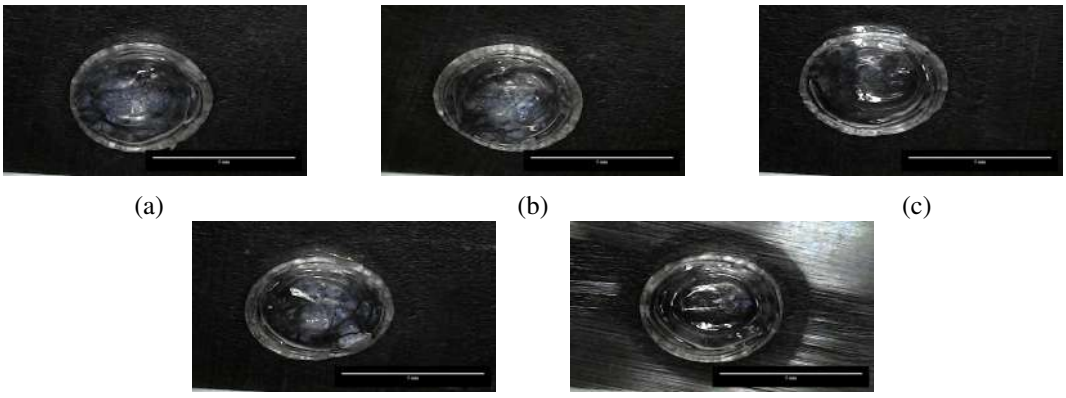

(a) (b) (c)

(d) (e)

Figure 4.12: Substrates scratched with 2000-grit sandpaper and treated for 7 seconds where (a) to (e) are Trials 1 to 5, respectively.

The resulting photomicrographs in Figure 4.12 are consistent with those found in Figures 4.10 and 4.11. A notable observation from among these photomicrographs is in Figure 4.12e, where there is an observable transparent area outside the melted area. It has a major axis length of 6.689 mm and a minor axis length of 5.457 mm.

The opacity of the melted areas for Figures 4.10, 4.11, and 4.12 decrease compared to those in Figures 4.3 to 4.9. This is related to the way that the treatment time is not directly proportional to the resulting surface roughness of the polymer [9]. The roughness of the polymer begins to increase with the same treatment time when the grit of the sandpaper used to scratch the substrate higher because its surface roughness is lower at the beginning.

The quantitative data collected from the USB Camera for the 7-second treatments are shown in Table 4.5. This table provides the same type of data as Table 4.3. Table 4.5 can be found in the next page.

Table 4.5: Length of the minor and major axes of the area treated for 7 seconds.

Grit	Trial	Melted		Translucent	
		Ma. Axis (mm)	Mi. Axis (mm)	Ma. Axis (mm)	Mi. Axis (mm)
1000	1	5.089	3.811	7.027	N/A
	2	5.138	3.739	7.018	4.759
	3	5.147	3.702	7.507	4.768
	4	4.972	3.802	6.536	4.346
	5	5.108	3.756	6.807	N/A
1500	1	5.028	3.778	N/A	N/A
	2	5.166	3.821	N/A	N/A
	3	5.212	3.644	N/A	4.850
	4	5.167	3.733	N/A	N/A
	5	5.212	3.671	7.270	4.541
2000	1	5.064	3.872	N/A	N/A
	2	5.283	3.769	N/A	N/A
	3	5.244	3.645	N/A	N/A
	4	5.256	3.640	N/A	N/A
	5	5.056	3.818	N/A	N/A

Some of the translucent parts of the treated area cannot be observed. Thus, to summarize these findings, there were all melted areas in the substrates of relatively high transparency. These melted areas had average dimensions of 5.143 mm $\times$ 3.747 mm for the major and minor axes, respectively. This gives an average area of 15.134 mm^2.

The findings for the 9-second treatments will be discussed. Figure 4.13 shows the photomicrographs taken of the samples that were scratched with a 1000-grit sandpaper and then treated for 9 seconds.

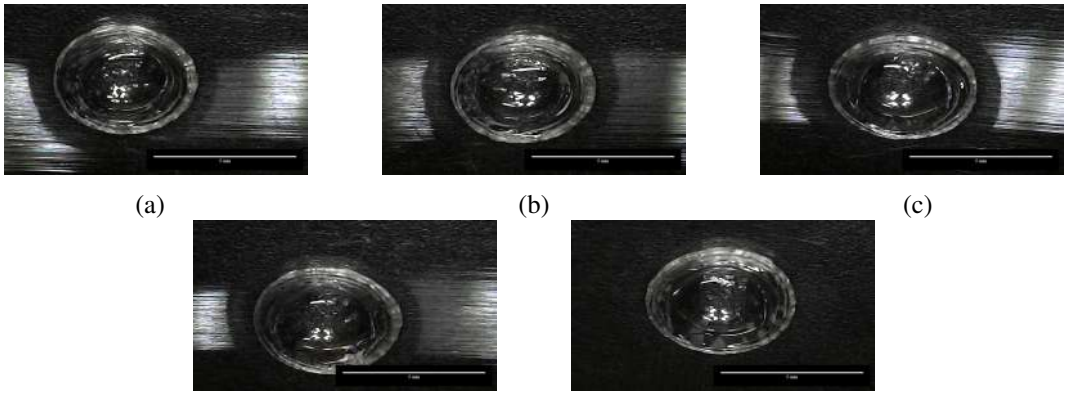

(a) (b) (c)

(d) (e)

Figure 4.13: Substrates scratched with 1000-grit sandpaper and treated for 9 seconds.

Figures 4.13a, 4.13b, 4.13c, and 4.13d display a transparent to translucent surrounding area to the melted area. However, the scratches were not wide enough to make measurements for the minor axis lengths of these transparent to translucent areas.

Moving on, Figure 4.14 shows the findings for the substrates scratched with a 1500-grit sandpaper.

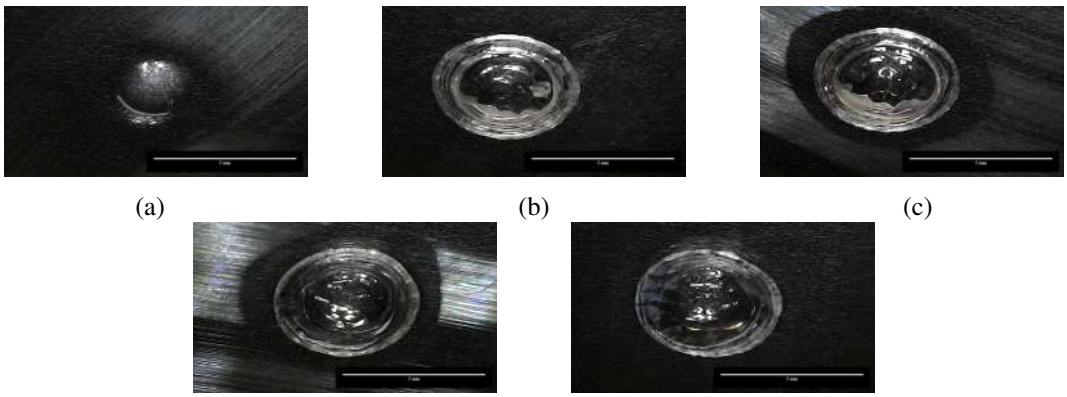

(a) (b) (c)

(d) (e)

Figure 4.14: Substrates scratched with 1500-grit sandpaper and treated for 9 seconds.

Most of these photomicrographs are similar to that shown in Figure 4.13, but not without some key differences. Figure 4.14a is different. This can also be attributed to the fact that this specific sample was treated on the same day as that in Figure 4.7e when the APPJ was not active for a longer amount of time. It is perhaps worth investigating further why the roughness within the melted area of Figure 4.14a is there. There are observably transparent areas surrounding the melted area found in Figures 4.14c and 4.14d. They have dimensions of 7.344 mm × 5.128 mm for Figure 4.14c and 7.087 mm × 5.503 mm for Figure 4.14d. These give areas of 29.578 mm^2 and 30.630 mm^2, respectively. For Figure 4.14e, there is an area of lower transparency of the left-hand side of the melted area alongside the reflected orange light within the melted area. This low transparency can also be attributed relation between the surface roughness and plasma treatment time, which is not directly proportional [9].

Finally, Figure 4.15 shows the resulting photomicrographs for the substrates treated for 9 seconds after being scratched with a 2000-grit sandpaper.

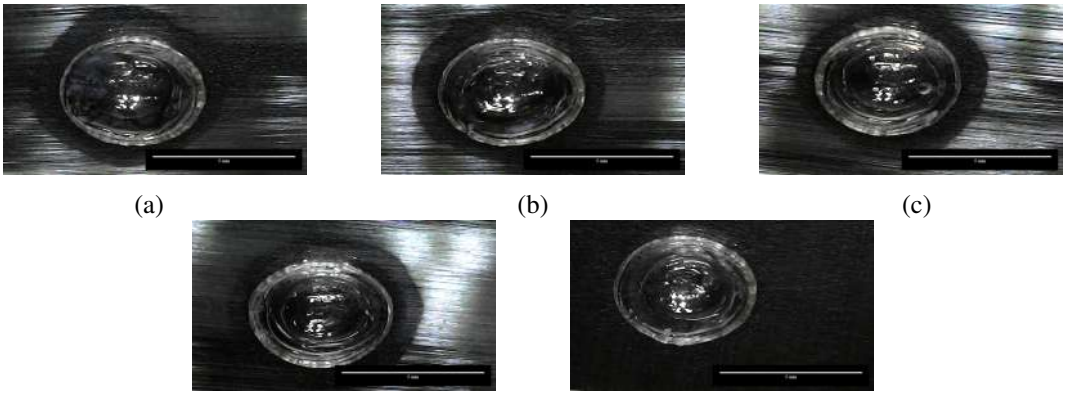

Figure 4.15: Substrates scratched with 2000-grit sandpaper and treated for 9 seconds.

Figures 4.15a and 4.15b exhibit some rough areas of PC within the melted areas' left-hand side and lower parts, respectively. Furthermore, Figures 4.15a and 4.15c have observable transparent areas surrounding the melted area. The dimensions of these transparent areas are 6.789 mm × 5.682 mm for Figure 4.15a and 6.816 mm × 5.474 mm for Figure 4.15c. These give the transparent parts areas of 30.297 mm^2 and 29.304 mm^2, respectively.

These findings for the 9-second treatments can be quantified as shown in Table 4.6 in the next page.

Table 4.6: Length of the minor and major axes of the area treated for 9 seconds.

Grit	Trial	Melted		Translucent	
		Ma. Axis (mm)	Mi. Axis (mm)	Ma. Axis (mm)	Mi. Axis (mm)
1000	1	5.089	3.845	6.589	N/A
	2	5.122	3.822	6.861	N/A
	3	5.202	3.681	7.390	N/A
	4	5.270	3.728	6.826	N/A
	5	5.274	3.808	N/A	N/A
1500	1	2.341	1.855	N/A	N/A
	2	5.221	3.680	N/A	N/A
	3	5.167	3.664	N/A	N/A
	4	5.130	3.836	N/A	N/A
	5	5.085	3.783	N/A	N/A
2000	1	5.170	3.807	N/A	N/A
	2	5.156	3.767	6.778	5.400
	3	5.167	3.825	N/A	N/A
	4	5.033	3.712	6.917	5.427
	5	5.024	3.795	N/A	N/A

The average area of the melted region based on its average dimensions can be found. With average dimensions of 4.963 mm as the length of the major axis and 3.641 mm as the length of the minor axis, which results in an area of 14.192 mm^2.

The melting of the PC substrate for high temperatures can be explained by the concept of the glass transition temperature (T_g). PC can withstand operating temperatures of 125 °C while also withstanding brief exposure of up to 150°C [30]. Prolonged exposure at temperatures part 125 °C lead to deformations in the PC substrate. Table 4.7 shows the plasma temperatures reached for each treatment time.

Table 4.7: Measured plasma temperatures at each treatment time.

Treatment Time (s)	Plasma Temperature (°C)
3	105.0
5	140.2
7	186.1
9	212.5

With the high temperatures measured for the plasma, this provides an explanation why the PC substrates exhibited melting after longer treatment times.

Surface roughness is generally an indication of high coefficient of friction [31]. The scratches made by the sandpaper on the surface of the PC substrates indicate an increased coefficient of friction. Because plasma treatment can increase the smoothness of a polymer [9] or decrease the coefficient of friction of thermoplastics [23], it is this mechanism of smoothening that reduces the scratching on the surface of the substrate and increases optical clarity. This smoothening mechanism may be a chemical process with the intensifying of the C−O and C=O bonds similar to that seen in [23]. However, due to the chemical resistance of PC, the effects observed in this study is mostly physical and caused by the temperature of the generated plasma, similar to that seen in one of the studies in Section 2.2 [24].

With the data collected from observations as well as those shown in Tables 4.1, 4.3, 4.5, and 4.6, statistical analysis is done in Section 4.4.

4.3 UV-Vis Transmittance Testing

Figure 4.16 shows the transmittance spectrum of a pristine PC substrate. It is noticeable that in the spectrum, majority of the wavelengths exhibit a 100% transmittance.

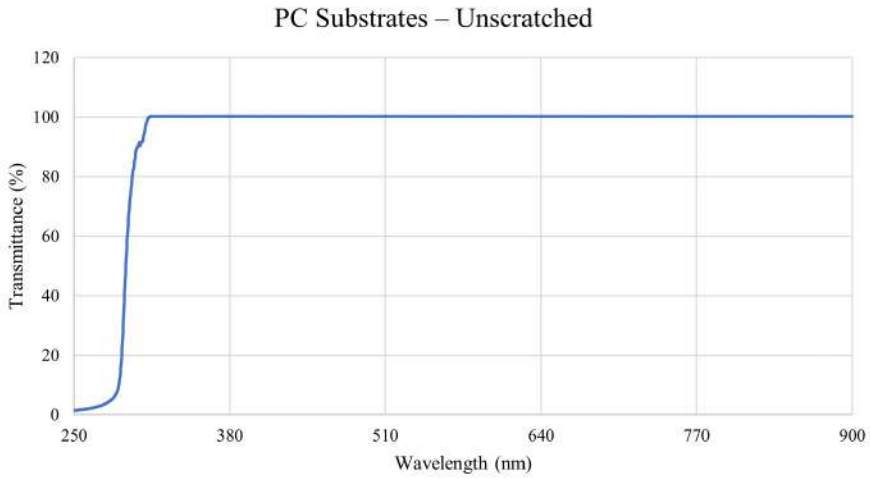

Figure 4.16: Transmittance spectrum of pristine PC substrate.

Figure 4.17 shows the transmittance spectra of five different substrates scratched with 1000-grit sandpaper.

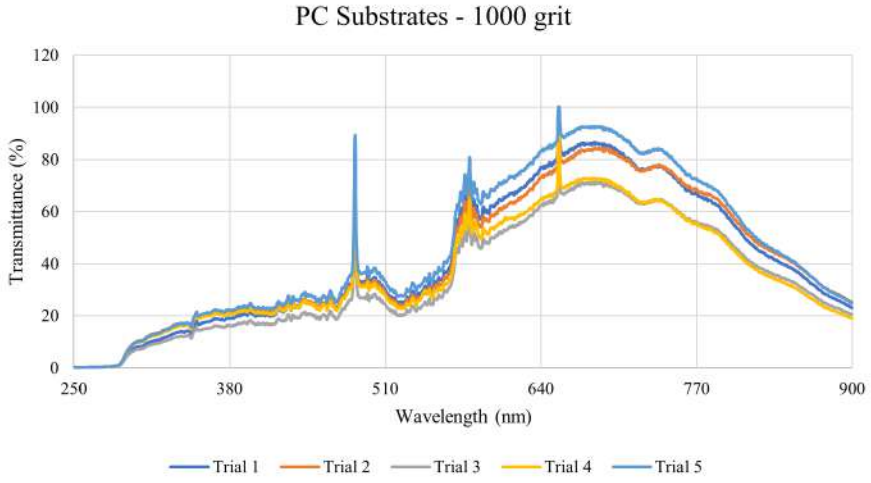

Figure 4.17: Transmittance spectrum of scratched PC substrate with 1000-grit sandpaper.

In Figure 4.17, similar shapes are being followed for all these transmittance spectra.

Figure 4.18 shows the transmittance spectra for the PC substrates scratched with 1500-grit sandpaper.

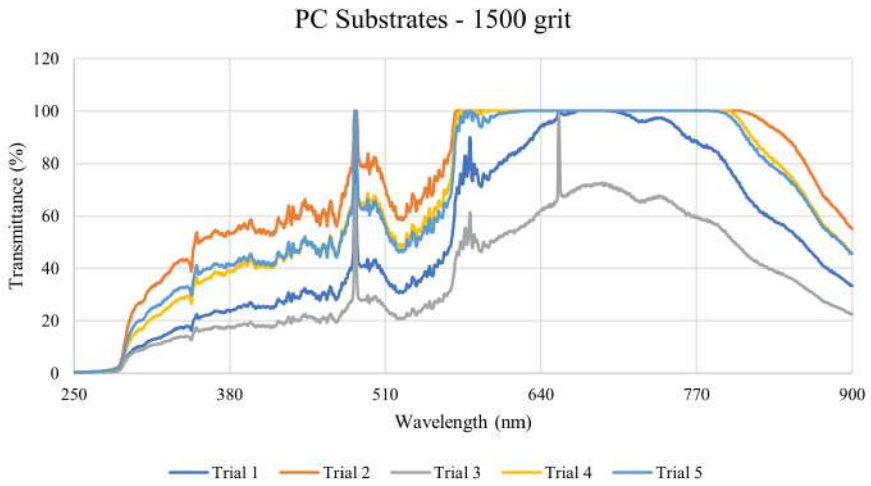

Figure 4.18: Transmittance spectrum of scratched PC substrate with 1500-grit sandpaper.

There is a less consistency in the spectra for each trial as shown in Figure 4.18. Trial 3 is more similar to the spectra found in Figure 4.17, whereas the other trials show higher transmittance values.

Figure 4.19 shows the spectra for five samples scratched with 2000-grit sandpaper.

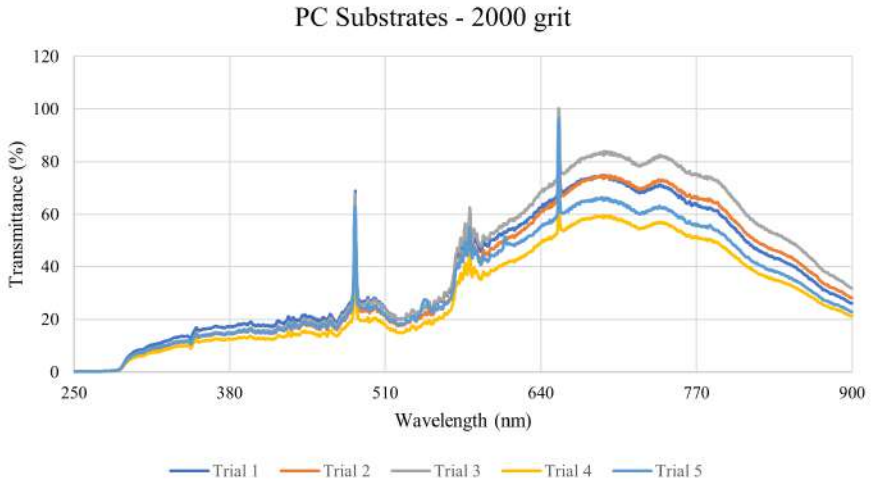

Figure 4.19: Transmittance spectrum of scratched PC substrate with 2000-grit sandpaper.

In Figure 4.19, the transmittance spectra for the substrates all follow the same general shape. The consistency and shape are shared qualities also found in the transmittance spectra for the substrates scratched with 1000-grit sandpaper in Figure 4.17.

The wavelengths of concern are with visible light, which is in the range of λ = 380 nm-750 nm [28]. This said, however, the range between λ = 380 nm-470 nm can come into question, but these data changes will be discussed in detail in Section 4.4.

Figure 4.20 on the next page shows the UV-Vis transmittance spectra for the substrates scratched with 1000-grit sandpaper and then treated for 3 seconds. These spectra follow the same trends.

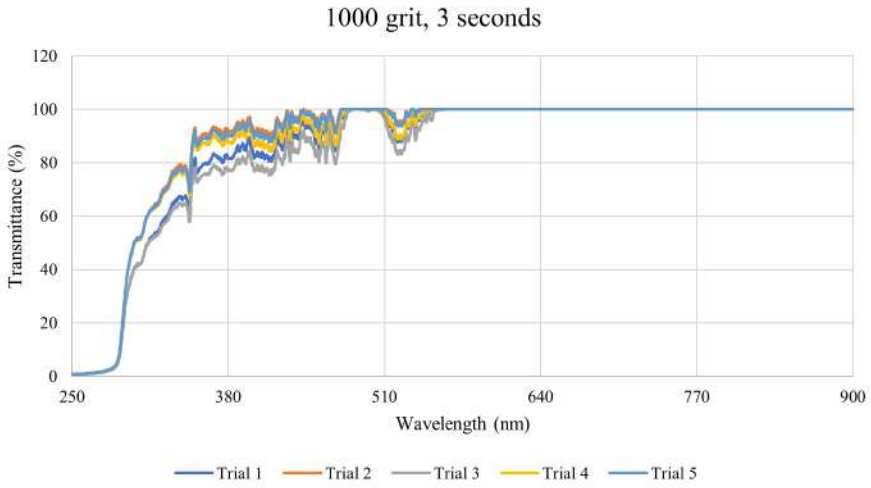

Figure 4.20: Transmittance spectrum of scratched PC substrate with 1000-grit sandpaper and then treated for 3 seconds.

Figure 4.21 shows the transmittance spectra for the substrates scratched with 1500-grit sandpaper with 3 seconds of APPJ treatment.

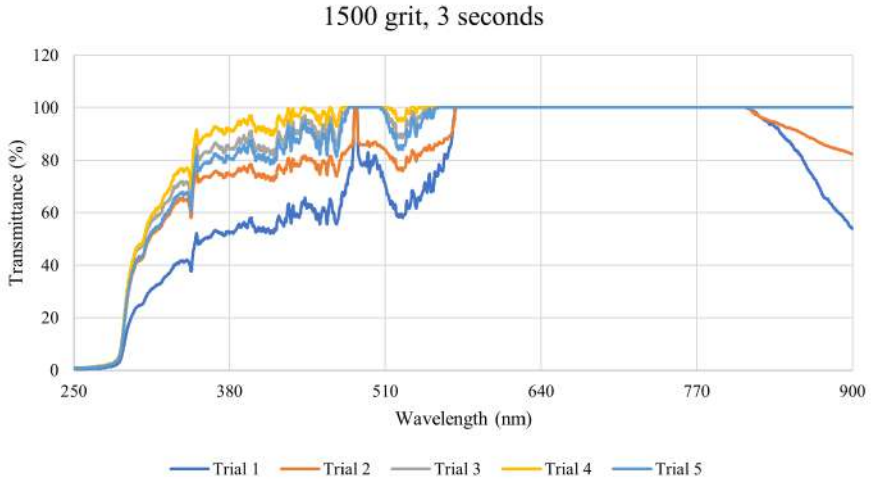

Figure 4.21: Transmittance spectrum of scratched PC substrate with 1500-grit sandpaper and then treated for 3 seconds.

The last treatments made for the 3-second treatments was done with the substrates scratched with 2000-grit sandpaper. Figure 4.22 shows the resulting transmittance spectra for these samples.

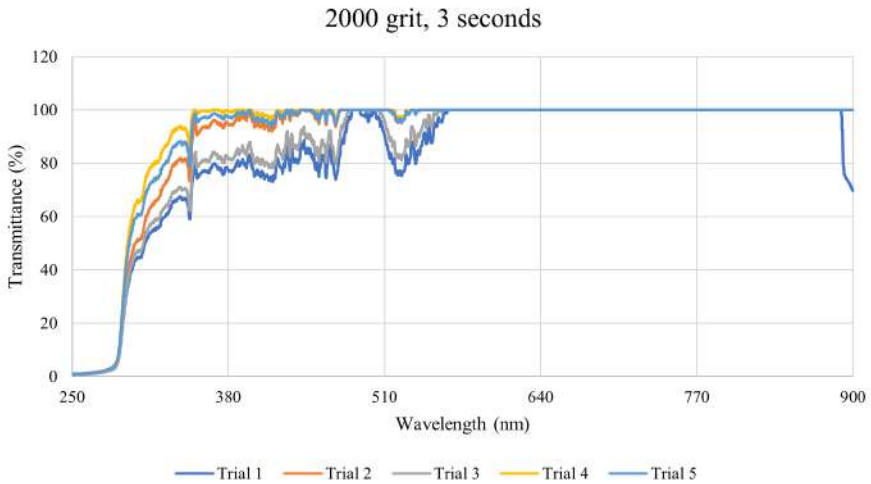

Figure 4.22: Transmittance spectrum of scratched PC substrate with 2000-grit sandpaper and then treated for 3 seconds.

The shapes of the individual spectra in Figure 4.22 are less consistent that those shown in Figures 4.20 and 4.21. However, the general shape of the spectra is still consistent with each other, while slightly differing from the spectra in Figures 4.20 and 4.21. The presence of three distinct and consistent dips in transmittance alongside the presence of a consistent peak are all noticeable differences that separate these spectra from the previous two.

Figure 4.23 shows the transmittance spectra for the substrates scratched with 1000-grit sandpaper then treated for 5 seconds.

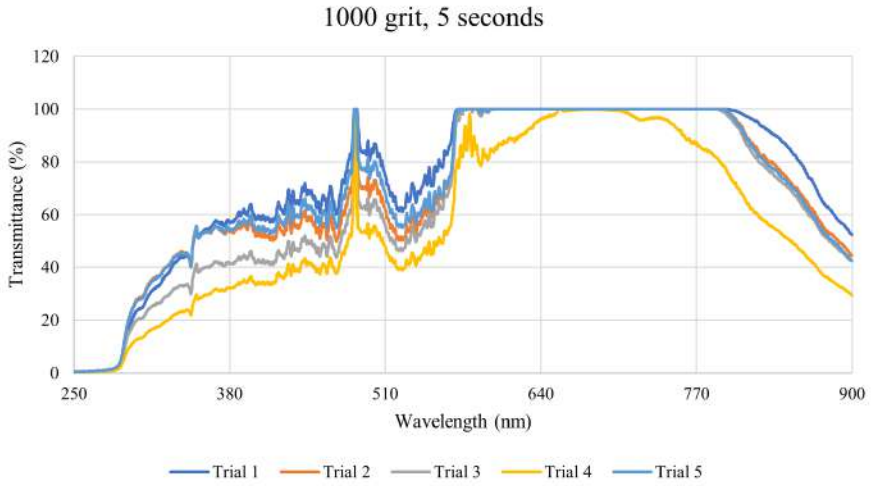

Figure 4.23: Transmittance spectrum of scratched PC substrate with 1000-grit sandpaper then treated for 5 seconds.

In Figure 4.7, the shape of the spectra remains consistent for different trials. There is one noticeable peak and one plateau for all these transmittance spectra. However, the spectrum for Trial 4 has a much narrower wavelength range for its plateau. Furthermore, it is the only one which displays a second peak.

Figure 4.24 shows the spectra for substrates scratched with 1500-grit sandpaper then treated for 5 seconds.

The shape of each spectra looks the same in this figure as well, though a noticeable deviation can be spotted in the spectrum for Trial 3.

Figure 4.25 shows the treatment for the substrate scratched with 2000-grit sandpaper then treated for 5 seconds.

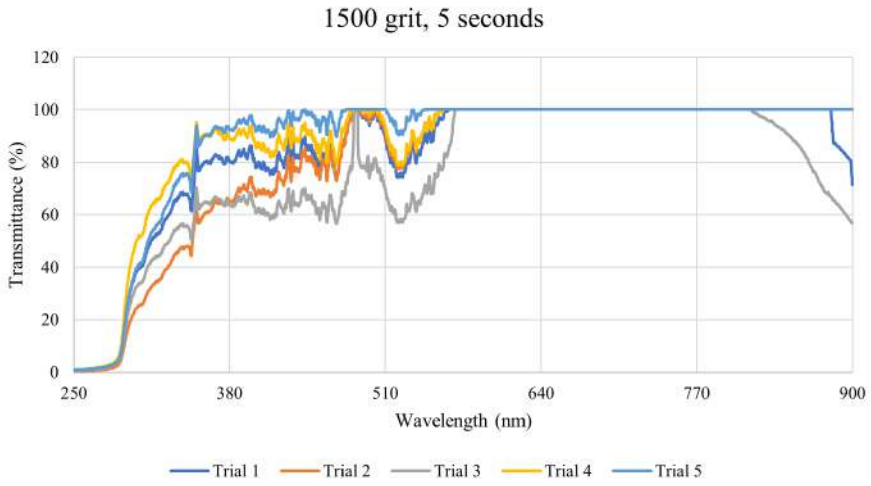

Figure 4.24: Transmittance spectrum of scratched PC substrate with 1500-grit sandpaper then treated for 5 seconds.

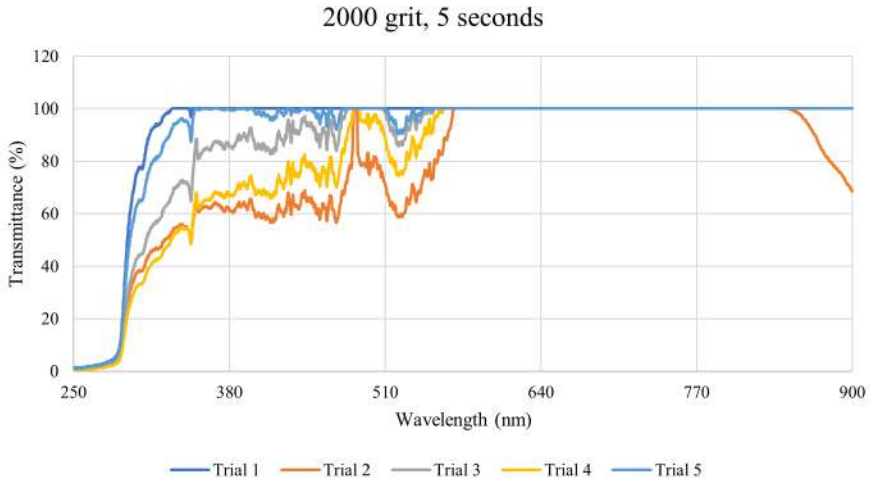

Figure 4.25: Transmittance spectrum of scratched PC substrate with 2000-grit sandpaper then treated for 5 seconds.

In Figure 4.9, Trial 1 acts as an outlier in terms of the shape since it has one plateau that spans to the end of the spectrum. However, Trials 2, 3, 4, and 5 are all similar to each other in terms of the trends that they follow.

The 7-second treatments will be discussed. Figure 4.26 show the transmittance spectra for the substrates scratched with 1000-grit sandpaper and treated for 7 seconds.

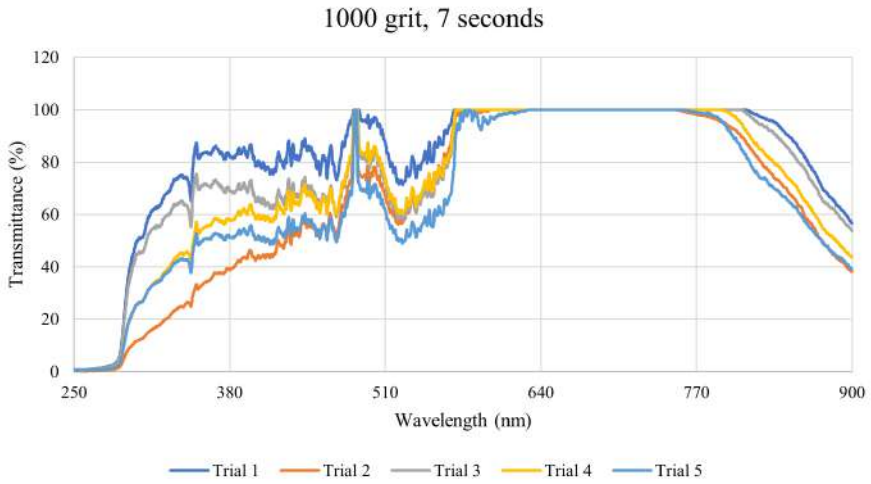

Figure 4.26: Transmittance spectrum of scratched PC substrate with 1000-grit sandpaper then treated for 7 seconds.

In Figure 4.26, all the spectra generally follow the same trend. There are no real outliers to speak of in this case.

Figure 4.27 in the next page shows the transmittance spectra for the substrates scratched with 1500-grit sandpaper and then treated for 7 seconds.

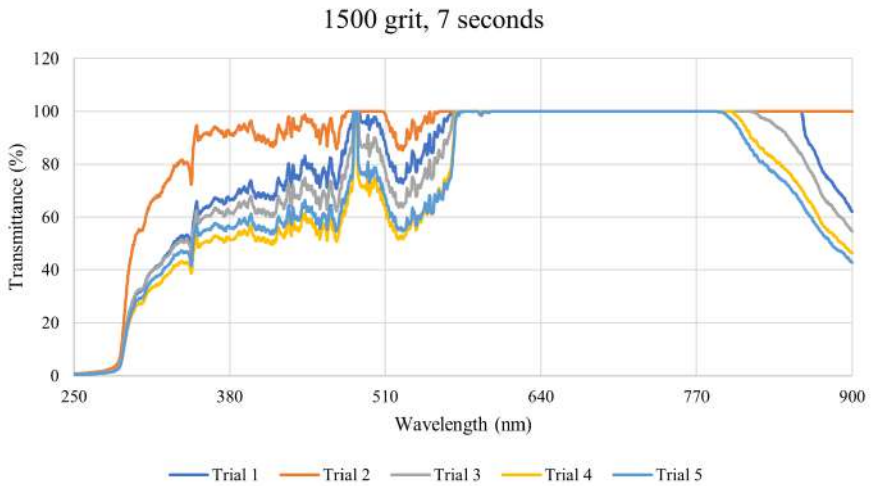

Figure 4.27: Transmittance spectrum of scratched PC substrate with 1500-grit sandpaper then treated for 7 seconds.

Trial 2 follows a slightly different trend since its first plateau is longer than the rest and its second plateau extends to the end of the spectrum. Aside from this, there are no other outlier spectra.

Figure 4.28 shows the transmittance spectra for the substrates scratched with 2000-grit sandpaper and then treated for 7 seconds.

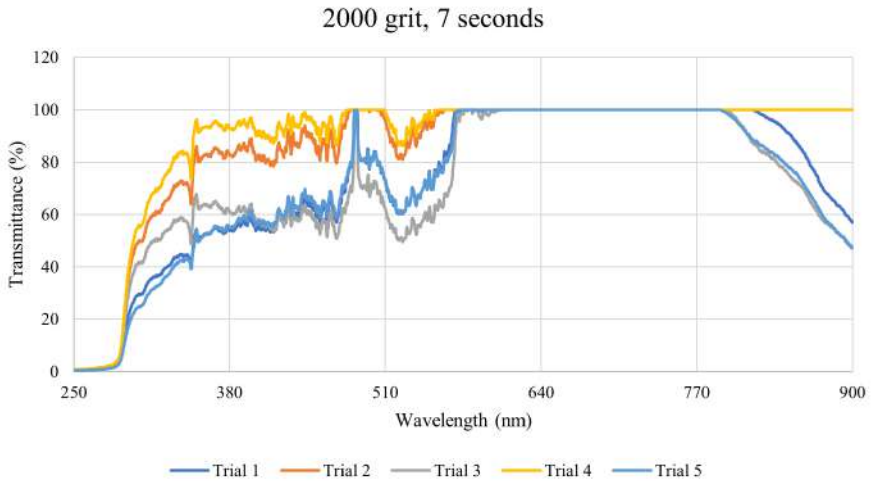

Figure 4.28: Transmittance spectrum of scratched PC substrate with 2000-grit sandpaper then treated for 7 seconds.

In Figure 4.28, Trials 2 and 4 follow almost the exact same trend while Trials 1, 3, and 5 also share the same trend.

For the final set of figures, the 9-second treatments will be examined. Figure 4.29 shows the transmittance spectra of the substrates scratched with 1000-grit sandpaper and then treated for 9 seconds.

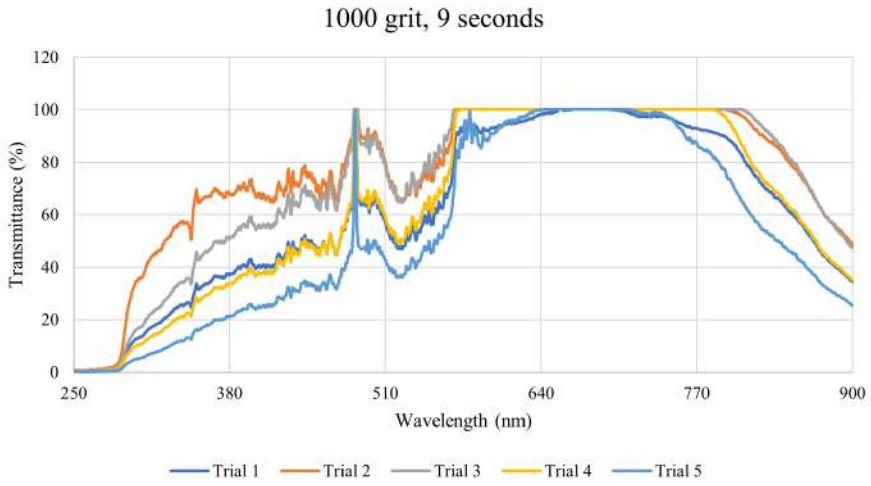

Figure 4.29: Transmittance spectrum of scratched PC substrate with 1000-grit sandpaper then treated for 9 seconds.

The trends that are followed for the spectra shown in Figure 4.29 are not consistent between trails. It is worth noting that specific peaks, valleys, and plateaus are consistent for these spectra nonetheless.

Figure 4.30 shows the transmittance spectra for the substrates scratched with 1500-grit sandpaper and then treated for 9 seconds.

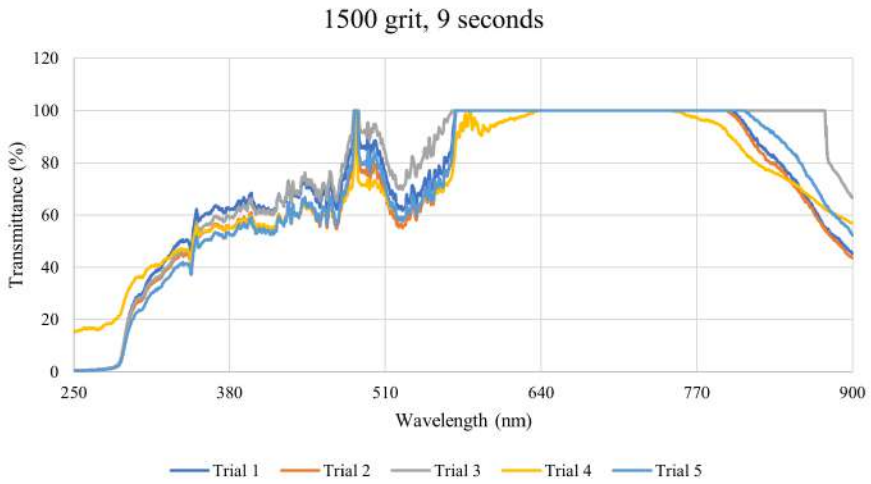

Figure 4.30: Transmittance spectrum of scratched PC substrate with 1500-grit sandpaper then treated for 9 seconds.

The spectra follow the same shape with consistency especially compared to Figure 4.29. However, the second plateau in Trial 4 is much shorter compared to the rest of the trials.

Finally, Figure 4.31 in the next page shows the transmittance spectra for the substrates treated for 9 seconds after being scratched with 2000-grit sandpaper.

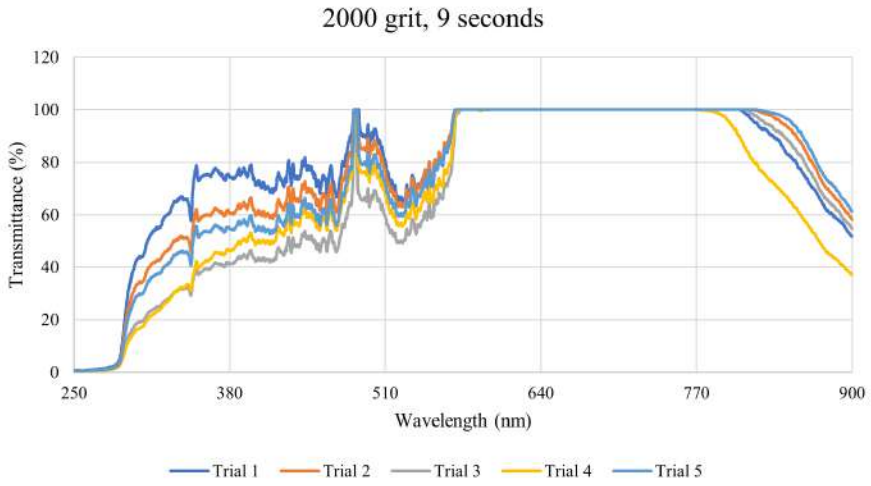

Figure 4.31: Transmittance spectrum of scratched PC substrate with 2000-grit sandpaper then treated for 9 seconds.

The trends that each spectrum follows remains consistent in each trial shown in Figure 4.31.

The data from the UV-Vis spectrometer allows analysis of the transmittance within the electromagnetic spectrum from the ultraviolet (UV) range to the infrared range. However, oversaturation of the UV-Vis spectrometer was observed within the visible spectrum towards the infrared range. As such, further analysis was given to the UV range analyzed by the spectrometer. The UV range refers to electromagnetic waves with wavelengths from 250 nm to 400 nm, though the range goes as low as 100 nm.

Figure 4.32 shows the transmittance spectrum of the pristine sample within the UV range.

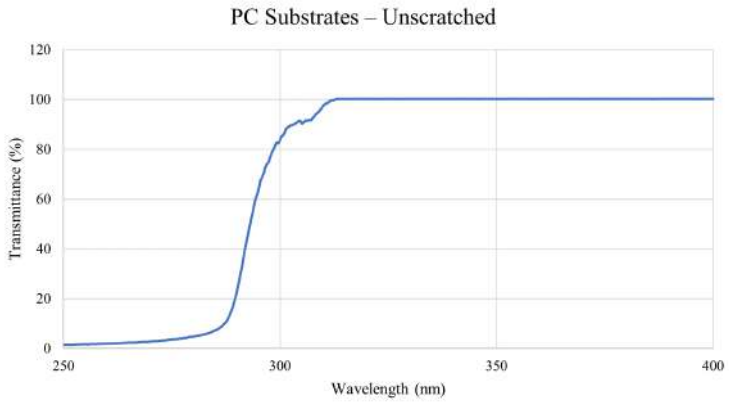

Figure 4.32: Transmittance spectrum of pristine PC substrate within the UV range.

As shown in Figure 4.32, there is already some part of the spectrum exhibiting oversaturation, but a high transmittance can be observed for majority of this part of the spectrum, nonetheless.

Figure 4.33 shows the transmittance spectra for the scratched samples. Note that each of the subfigures represent the different grits of sandpaper used to scratch the PC surface.

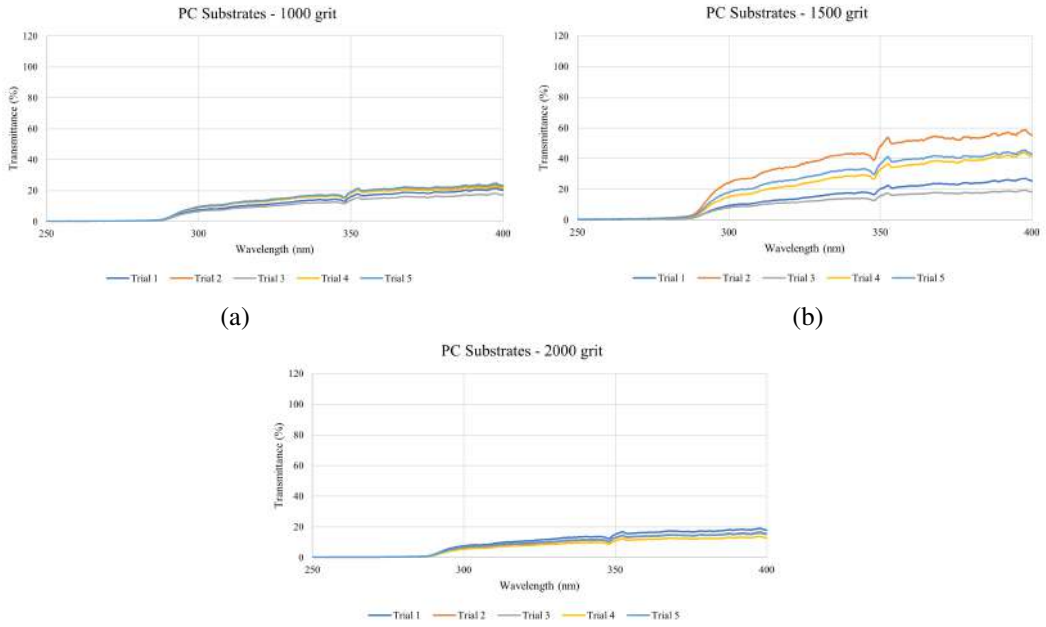

Figure 4.33: Transmittance spectrum of PC substrate scratched with (a) 1000-, (b) 1500-, and (c) 2000-grit sandpaper within the UV range.

Meanwhile, Figure 4.34 shows the spectra of all PC samples that were subject to different plasma treatment times after being scratched with 1000-grit sandpaper.

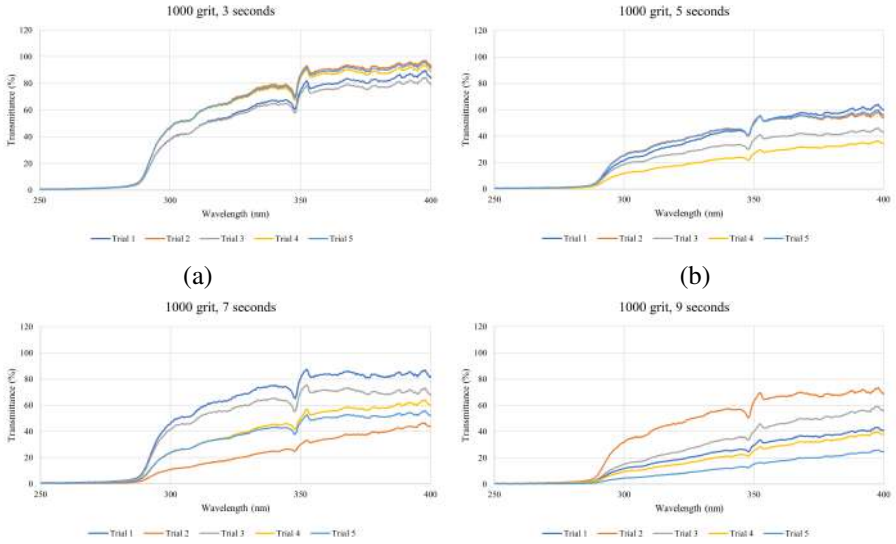

(a) (b)

(c) (d)

Figure 4.34: UV Transmittance spectrum of PC substrate scratched with 1000-grit sandpaper and then plasma treated for (a) 3, (b) 5, (c) 7, and (d) 9 seconds.

Figure 4.35 shows the transmittance spectra for all plasma treated PC substrates after scratching with 1500-grit sandpaper.

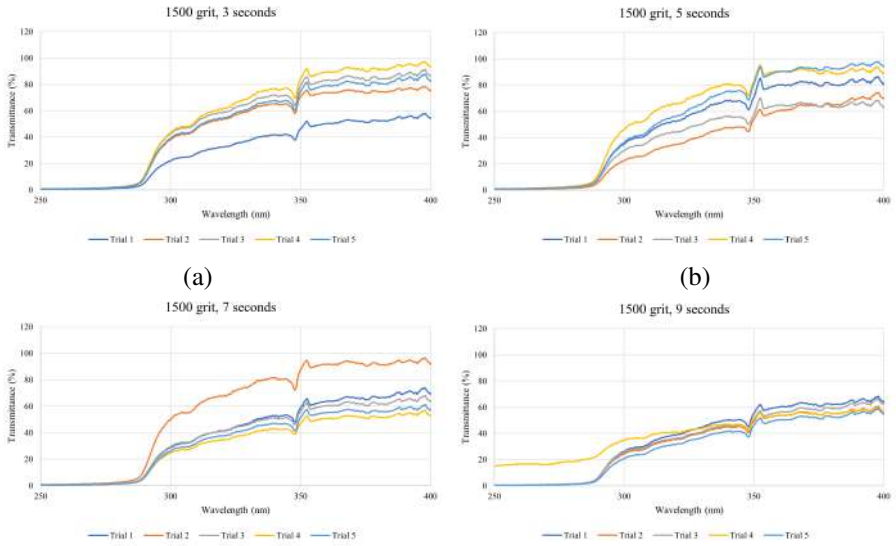

(a) (b)

(c) (d)

Figure 4.35: UV Transmittance spectrum of PC substrate scratched with 1500-grit sandpaper and then plasma treated for (a) 3, (b) 5, (c) 7, and (d) 9 seconds.

Finally, Figure 4.36 shows the transmittance spectra within the UV range of the PC substrates treated after scratching with 2000-grit sandpaper.

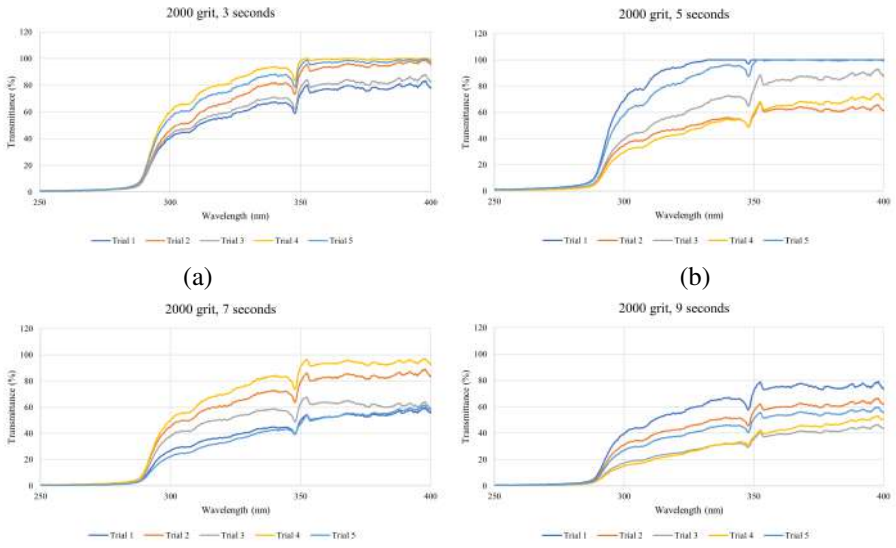

(a) (b)

(c) (d)

Figure 4.36: UV Transmittance spectrum of PC substrate scratched with 2000-grit sandpaper and then plasma treated for (a) 3, (b) 5, (c) 7, and (d) 9 seconds.

The transmittance data is further analyzed in Section 4.4.

4.4 Discussion

The first part of this section tackles the differences in the transparent area in relation to the treatment time. This was done by plotting the mean transparent area against the time for each grit. The plots are shown in Figure 4.37 in the next page alongside the error bars which represent one standard deviation from the mean value. For the first graph, it may be observed that the 3-second treatments exhibited the best results in terms of transparent area. For the second graph, a plateau can be observed, but an increase in transparent area can be observed with increasing treatment time. For the third graph, an initial dip in transparent area can be observed after 3 seconds of treatment, after which the size of the transparent area increases with time.

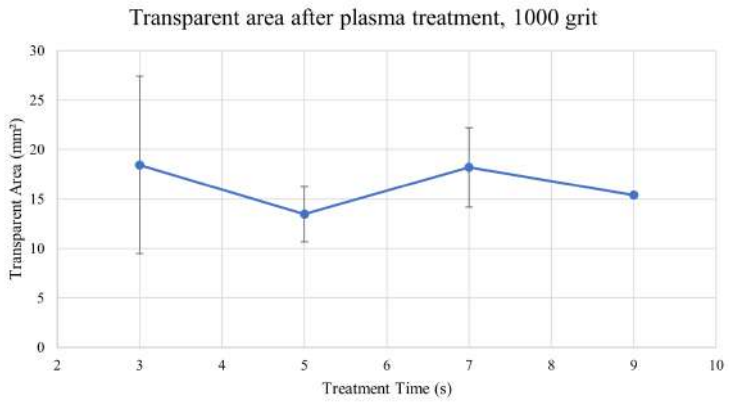

(a)

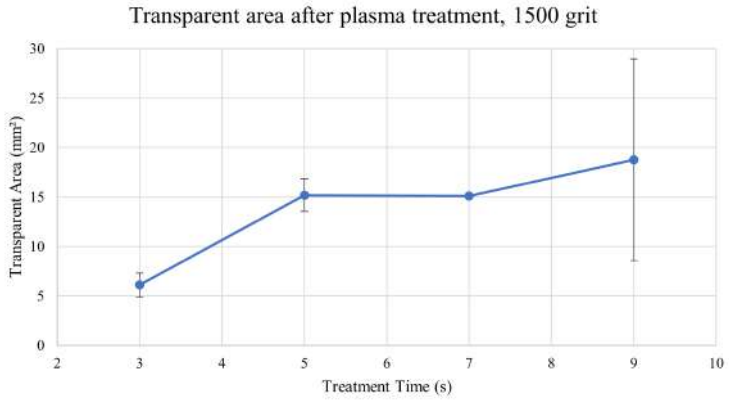

(b)

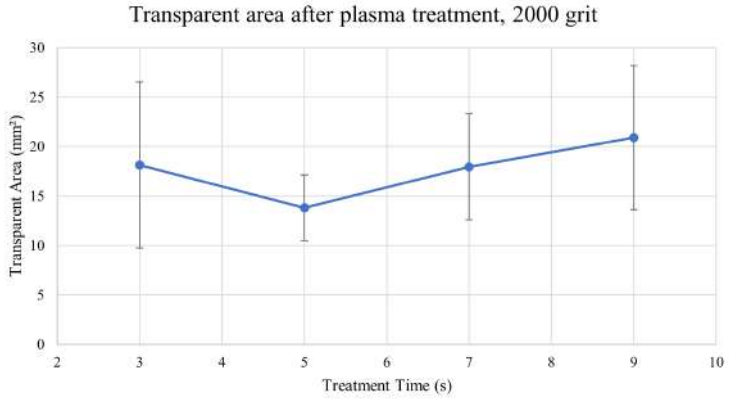

(c)

Figure 4.37: Plot of mean transparent area vs. treatment time for substrates scratched with (a) 1000-grit, (b) 1500-grit, and (c) 2000-grit.

Based on these graphs, there is no observably consistent pattern relating the size of the transparent area to the treatment time.

Plotted in Figure 4.38 is the plot of the mean area under the curve for each trial among the substrates scratched with 1000-grit sandpaper against treatment time. Alongside this plot are error bars, representing one standard deviation from each of the mean values.

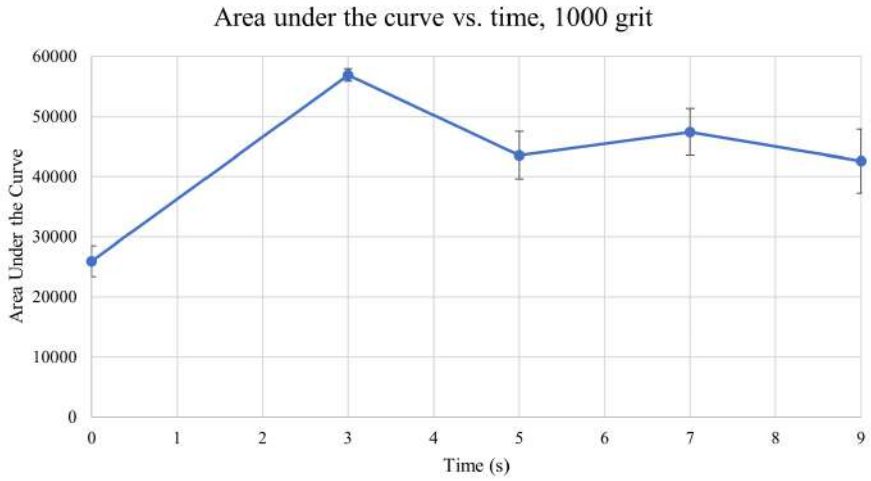

Figure 4.38: Plot of the mean area under the spectrum vs. time for the substrates scratched with 1000-grit sandpaper.

In Figure 4.38, it can be observed that the relation of the area under the transmittance curve to time is not linear. Visually, the 3-second treatment exhibited the best and most consistent results, as shown by the peak in the mean area under the transmittance curve and the smallest error bars. As such, the 3-second treatment was determined to be the optimal treatment time in this case.

Figure 4.39 also shows the plot of the mean area under the transmittance curve against treatment time.

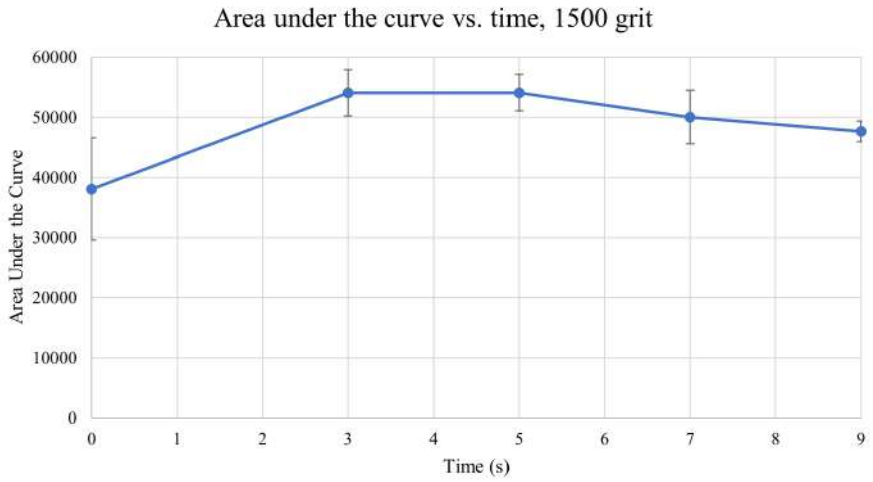

Figure 4.39: Plot of the mean area under the spectrum vs. time for the substrates scratched with 1500-grit sandpaper.

In Figure 4.39, the best treatment time among the ones used in this study was the 3-second treatment time, which is where the area under the transmittance curve peaked. However, its consistency is less than that shown in Figure 4.38, as shown by its larger error bars.

Figure 4.40 shows the plot of the mean area under the curve for each trial among the substrates scratched with 2000-grit sandpaper against treatment time.

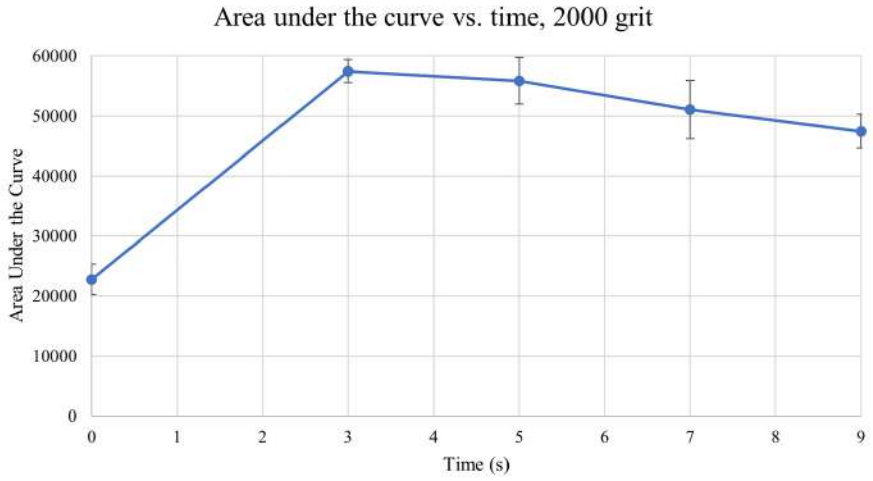

Figure 4.40: Plot of the area under the spectrum vs. time for the substrates scratched with 2000-grit sandpaper.

In Figure 4.40, the best treatment time among the ones used in this study was the 3-second treatment time with excellent consistency, as shown by the peak in the area of the transmittance curve at 3 seconds and the small error bar shown.

All these areas are consolidated with their averages in Table 4.8. On average, the highest increase in the area under the curve compared to the untreated samples is found in the 3-second treatments, which agree with the data collected in Figures 4.38 to 4.40.

Table 4.8: Consolidated table of average area under each spectrum.

Treatment Time (s)	Grit	Average area under the curve
0	1000	25903.14187
	1500	38081.73252
	2000	22767.53477
3	1000	56917.17526
	1500	54077.12765
	2000	57465.30156
5	1000	43557.81883
	1500	54143.70851
	2000	55860.57193
7	1000	47423.51571
	1500	50061.31371
	2000	51092.19848
9	1000	42570.97907
	1500	47676.94755
	2000	47450.79155

The highest average increase in the area under the curve were observed for the 3-second treatments. Furthermore, the regression lines in Figures 4.38 to 4.40 showing that the optimal treatment times were all closest to 3 seconds. These are good indications that the treatment time of 3 seconds provided the best results.

The spectrum shown in Figure 4.16 has an area under the curve of 60810.99328. Table 4.9 shows the average difference in the area under the curve for each treatment time.

Table 4.9: Average differences in the area under the curve compared to the pristine sample.

Treatment Time (s)	Difference in area
0	31893.52357
3	4657.791790
5	9623.626857
7	11285.31732
9	14911.42056

As shown in Table 4.9, the substrates treated for 3 seconds showed the least difference in the area under the curve compared to the pristine sample. This is even further proof that the 3-second treatment remains the optimal treatment time among the selected treatment times. Furthermore, this difference is much smaller compared to the spectra of the samples treated for 5, 7, and 9 seconds.

For data available strictly within the UV range, the following data in Table 4.10 shows the area under the curve within the wavelengths of 250 nm and 400 nm. It is important to note in this case that the area within this same range of wavelengths for the pristine sample is 10708.55461.

Table 4.10: Consolidated table of average area under each spectrum within the UV range.

Treatment time (s)	Grit	Average area under the curve
0	1000	1705.691044
	1500	3021.607790
	2000	1281.319410
3	1000	7823.302570
	1500	6915.581440
	2000	8423.560072
5	1000	4171.752372
	1500	6942.506966
	2000	7886.692172
7	1000	5420.528788
	1500	5918.647284
	2000	6410.838192
9	1000	3438.857280
	1500	5159.967338
	2000	4944.946442

As shown in Table 4.10, none of the values are close to the area under the curve of the pristine sample. However, a noticeable decrease in difference can be seen for the 3-second treatments. This is further exposed by the data in Table 4.11.

Table 4.11: Average difference in the area under the curve against the pristine sample.

Treatment Time (s)	Difference in area
0	8705.681862
3	2987.739916
5	4374.904107
7	4791.883189
9	6193.964257

Based on the data in Table 4.11, the smallest average difference in area under the spectrum is found for samples treated for 3 seconds, with a steady increase as treatment time increases. As such, the best results are found at 3 seconds of plasma treatment.

Chapter 5

Conclusions and Recommendations

5.1 Conclusions

The PC substrates were scratched with 1000-, 1500-, and 2000-grit sandpaper with a constant force of 14.7 N. After plasma treatment using an air APPJ, the scratches were successfully removed as shown by the significant increase in transmittance as well as from macroscopic inspection.

The macroscopic inspections show that the treated area is generally elliptical in shape with a transparent center. This transparent area either becomes translucent in a stepwise manner or becomes opaque completely after some distance from the center is reached. Treatments of greater than 3 seconds were also shown to have formed deformations within the transparent area. This implies that there is a change in the optical focal point of the substrate which is not a good result considering that the applications of face shields require the user to see things accurately. Furthermore, the areas of the different transparent areas were measured and the average area of these transparent parts was approximately 15.954 mm^2. Lastly, the transparent areas and treatment time were plotted to find whether any correlation existed where it was found that the substrates scratched with 1000- and 2000-grit sandpaper exhibited negligible correlation in terms of the transparent area with time whereas the substrate scratched with 1500-grit sandpaper exhibited a moderate positive correlation.

The UV-Vis transmittance spectra were also gathered for each treated substrate as well as for the scratched substrates. While no real data was found here outside the data analysis part, it was shown that specific wavelengths of electromagnetic waves were transmitted even in supposedly opaque substrates. The area under the transmittance curves were taken and analyzed in relation to both the pristine substrate and the scratched, untreated substrates. Both comparisons showed that the 3-second treatment

was the most effective in scratch removal and, consequently, increasing optical clarity. Comparisons strictly within the UV range of waves also showed that the 3-second treatment provided the most improvement in transmittance of waves. Furthermore, considering the changes in the focal point of the substrates as observed due to the melting of the substrate, the conclusion of this study is that 3-second treatments produced the best results in terms of maximizing the transmittance and displaying minimal changes in other optical properties of the substrate.

5.2 Recommendations

The following recommendations are advised for future researchers who are interested in deepening this line of work.

Keeping the way one scratches the substrates consistent is highly recommended. The setup used in the latter part of the study is suggested since it provides a more even scratching opacity compared to the setup shown in the Figure in Chapter 3. This will help reduce any possible errors that may have happened in this study especially considering the data for the substrates scratched with 1500-grit sandpaper.

The usage of a scanning method, that is, adjusting the position of either the plasma jet or the substrate throughout the treatment to more evenly treat the surface of the substrate is also recommended. The researchers suggest automating this method because doing this manually is likely prone to human error. Furthermore, the results of the study may also likely be attributed to momentum-based changes instead of thermally-induced changes because melting can be completely prevented.

Another recommendation is to replicate the study with differences in specific variables. This study has a strict scope, setting only the treatment time as an independent variable with the rest of the variables being constant. Lower grit of sandpaper and/or more force is suggested if the researcher wants to study with deeper scratches. For different plasma parameters, it is recommended to try treatment of substrates with either a different gas pump (such as Ar or N_2), different nozzle distances, and/or different voltage. Another recommendation related to this will be expounded on later.

It is also recommended to conduct material analysis immediately upon plasma treatment. This allows researchers to find out what chemical mechanisms may be happening to the PC substrates. Different methods such as X-ray Photoelectron Spectroscopy (XPS), Fourier Transform Infrared Spectroscopy (FTIR), and the usage of either an Atomic Force Microscope (AFM) or a Scanning Electron Microscope (SEM).

Another recommendation is to use atmospheric plasma treatment for different polymers for these applications. Specifically, polymethylmethacrylate (PMMA) is used in optical applications alongside PC. Trying atmospheric plasma treatment for scratches on polymers used for lenses is a recommended line to follow. The thickness of the polymers used in these studies may also affect the problem shown in this study with the deformation of the material.

It is also recommended that UV-Vis spectrometry be redone, specifically for the visible spectrum. This is because oversaturation was observed within the data, characterized by a flat-lining of the transmittance values. As such, a rerun UV-Vis spectrometry is recommended with particular focus on finding data within the visible spectrum to provide more complete data.

Finally, the resulting transparent area of the treatments is very small compared to the size of the substrate. With this in mind, it is recommended to also try this study with glow discharge plasma instead. This may resolve the problem with the unevenness of the removal of the scratches. This may allow for the treatment of larger substrates compared to those used in this study.

References

[1] J. Bittencourt, *Fundamentals of Plasma Physics*, 3rd ed. New York, USA: Springer, 2004, ch. 1. [Online]. Available: https://link.springer.com/book/10.1007/978-1-4757-4030-1

[2] C. Tendero, C. Tixier, P. Tristant, J. Desmaison, and P. Leprince, "Atmospheric pressure plasmas: A review," *Spectrochimica Acta Part B: Atomic Spectroscopy*, vol. 61, no. 1, pp. 2–30, 2006. [Online]. Available: https://www.sciencedirect.com/science/article/pii/S0584854705002843

[3] M. Keidar and I. I. Beilis, *Plasma Engineering*, 2nd ed. Academic Press, 2018, ch. 1. [Online]. Available: https://www.sciencedirect.com/science/article/pii/B9780128137024000016

[4] P. Bellan, *Fundamentals of Plasma Physics*. Cambridge, UK: Cambridge University Press, 2006, ch. 1. [Online]. Available: https://www.cambridge.org/core/books/fundamentals-of-plasma-physics/4E88EC98AA7339A290AD0734641A7970

[5] U. Kogelschatz, "Atmospheric-pressure plasma technology," *Plasma Physics and Controlled Fusion*, vol. 46, no. 12B, nov 2004. [Online]. Available: https://dx.doi.org/10.1088/0741-3335/46/12B/006

[6] D. Braný, D. Dvorská, E. Halašová, and H. Škovierová, "Cold atmospheric plasma: A powerful tool for modern medicine," *International Journal of Molecular Sciences*, vol. 21, 2020.

[7] M. M. M. Mendoza, C. L. S. Mahinay, C. J. D. Cruz, and R. A. Guerrero, "Production of plasma-activated water using an atmospheric pressure plasma jet system," Undergraduate Thesis, Ateneo de Manila University, Quezon City, Metro Manila, Philippines, 2022.

[8] C. J. P. Zafra, P. V. T. Ramos, I. B. Culaba, and C. L. S. Mahinay, "Enhanced wettability of polycarbonate (PC) and adhesion with aluminum by atmospheric-pressure plasma jet treatment," Undergraduate Thesis, Ateneo de Manila University, Quezon City, Metro Manila, Philippines, 2019.

[9] T. Homola, J. Matoušek, B. Hergelová, M. Kormunda, L. Y. L. Wu, and M. Černák, "Activation of poly(methyl methacrylate) surfaces by atmospheric pressure plasma," *Polymer Degradation and Stability*, no. 97, pp. 886 – 892, 2012. [Online]. Available: https://www.sciencedirect.com/science/article/pii/S0141391012001073?via%3Dihub

[10] L. R. B. Salazar, C. L. S. Mahinay, I. B. Culaba, and J. M. A. Diaz, "Wettability characteristics of copper surfaces treated with air plasma using atmospheric pressure plasma jet (APPJ)," Undergraduate Thesis, Ateneo de Manila University, Quezon City, Metro Manila, Philippines, 2022.

[11] I. E. Echaluse and C. L. S. Mahinay, "Surface modification of polytetrafluoroethylene (PTFE) through atmospheric pressure plasma jet treatment," Undergraduate Thesis, Ateneo de Manila University, Quezon City, Metro Manila, Philippines, 2020.

[12] W. D. Callister and D. G. Rethwisch, *Materials Science and Engineering*, 10th ed. New York City, NY: Wiley & Sons, 2018. [Online]. Available: https://www.wiley.com/en-us/Materials+Science+and+Engineering%3A+An+Introduction%2C+10th+Edition-p-9781119405498

[13] D. Kyriacos, *Plastics Materials*, 8th ed. Oxford, UK: Butterworth-Heinemann, 2017, ch. 17. [Online]. Available: https://www.sciencedirect.com/science/article/pii/B9780323358248000177?via%3Dihub

[14] Blue Eagle Safety, "Face shields – why you should always choose polycarbonate visors rather than PVC?" [Online]. Available: https://blueeagle-safety.com/face-shield-why-polycarbonate-visor/

[15] 3M, "3M^{TM} Clear Polycarbonate Faceshield WP96, 82701-00000, Molded, 10 EA/Case." [Online]. Available: https://www.3mphilippines.com.ph/3M/en_PH/p/d/v0000577733/

[16] J. M. G. Cowie and V. Arrighi, *Polymers: chemistry and physics of modern materials*. CRC Press, 2007, ch. 1: Introduction.

[17] D. Hegemann, H. Brunner, and C. Oehr, "Plasma treatment of polymers for surface and adhesion improvement," *Nuclear Instruments and Methods in Physics Research B*, vol. 208, pp. 281–286, 2003.

[18] A. Hofrichter, P. Bulkin, and B. Drévillon, "Plasma treatment of polycarbonate for improved adhesion," *Journal of Vacuum Science and Technology A*, vol. 20, no. 245, 2002. [Online]. Available: https://avs.scitation.org/doi/10.1116/1.1430425

[19] B. W. Muir, S. L. M. Arthur, H. Thissen, G. P. Simon, H. J. Griesser, and D. G. Castner, "Effects of oxygen plasma treatment on the surface of bisphenol A polycarbonate: a study using SIMS, principal component analysis, ellipsometry, XPS and AFM nanoindentation," *Surface and Interface Analysis*, no. 38, pp. 1186 – 1197, 2006. [Online]. Available: https://analyticalsciencejournals.onlinelibrary.wiley.com/doi/abs/10.1002/sia.2363

[20] O. V. Penkov, M. Khadem, W.-S. Lim, and D.-E. Kim, "A review of recent applications of atmospheric pressure plasma jets for materials processing," *Journal of Coatings Technology and Research*, no. 12, pp. 225 – 235, 2015. [Online]. Available: https://link.springer.com/article/10.1007/s11998-014-9638-z

[21] A. Qureshi, S. Shah, S. Pelagade, N. L. Singh, S. Mukherjee, A. Tripathi, U. P. Despande, and T. Shripathi, "Surface modification of polycarbonate by plasma treatment," in *23rd National Symposium on Plasma Science & Technology*, no. 208. IOP Publishing, 2010. [Online]. Available: https://iopscience.iop.org/article/10.1088/1742-6596/208/1/012108/pdf

[22] C. B. Mello, K. G. Kostov, M. Machida, L. R. O. de Oliveira Hein, and K. A. de Campos, "Surface modification of polycarbonate by atmospheric-pressure plasma jets," *IEEE Transactions on Plasma Science*, vol. 40, no. 11, 2012. [Online]. Available: https://doi.org/10.1109/TPS.2012.2210055

[23] J. G. F. Abalos and C. L. S. Mahinay, "Tribological properties of surface plasma treated thermoplastic polymers using an atmospheric pressure plasma jet," Quezon City, Metro Manila, Philippines, 2019.

[24] M. Noeske, J. Degenhardt, S. Strudthoff, and U. Lommatzsch, "Plasma jet treatment of five polymers at atmospheric pressure: surface modifications and the relevance for adhesion," *International Journal of Adhesion & Adhesives*, no. 24, pp. 171 – 177, 2004. [Online]. Available: https://www.sciencedirect.com/science/article/abs/pii/S0143749603001246?via%3Dihub

[25] Z. Chen, T. G. Deutsch, H. N. Dinh, K. Domen, K. Emery, A. J. Forman, N. Gaillard, R. Garland, C. Heske, T. F. Jaramillo, A. Kleiman-Shwarsctein, E. Miller, K. Takanabe, and J. Turner, *UV-Vis Spectroscopy*. New York, NY: Springer New York, 2013, pp. 49 – 62. [Online]. Available: https://link.springer.com/chapter/10.1007/978-1-4614-8298-7_5

[26] Z. Navrátil, D. Trunec, R. Šmíd, and L. Lazar, "A software for optical emission spectroscopy - problem formulation and application to plasma diagnostics," *Czechoslovak Journal of Physics*, vol. 56, 2006. [Online]. Available: https://link.springer.com/article/10.1007/s10582-006-0308-y

[27] C. E. R. Petilla, *RStudio Manual for High School Researches*. Sto Niño, Tugbok Dist., Davao City: Philippine Science High School - Southern Mindanao Campus, 2022, ch. 6: Correlation.

[28] R. A. Freedman, H. D. Young, and A. L. Ford, *University Physics with Modern Physics*. Addison-Wesley, 2012, ch. 32: Electromagnetic Waves.

[29] H. van der Rhee, E. de Vries, C. Coomans, P. van de Velde, and J. W. Coebergh, "Sunlight: For better or for worse? a review of positive and negative effects of sun exposure," *Cancer Research Frontiers*, vol. 2, no. 2, pp. 156 – 183, 2016.

[30] R. Wehrmann, *Encyclopedia of Materials: Science and Technology*. Elsevier, 2001, ch. Polycarbonate, pp. 7149 – 7151.

[31] J. O. Ajayi, "Fabric smoothness, friction, and handle," *Textile Research Journal*, vol. 62, no. 1, pp. 52 – 59, 1992.

Appendix A

Calibration scale for USB camera

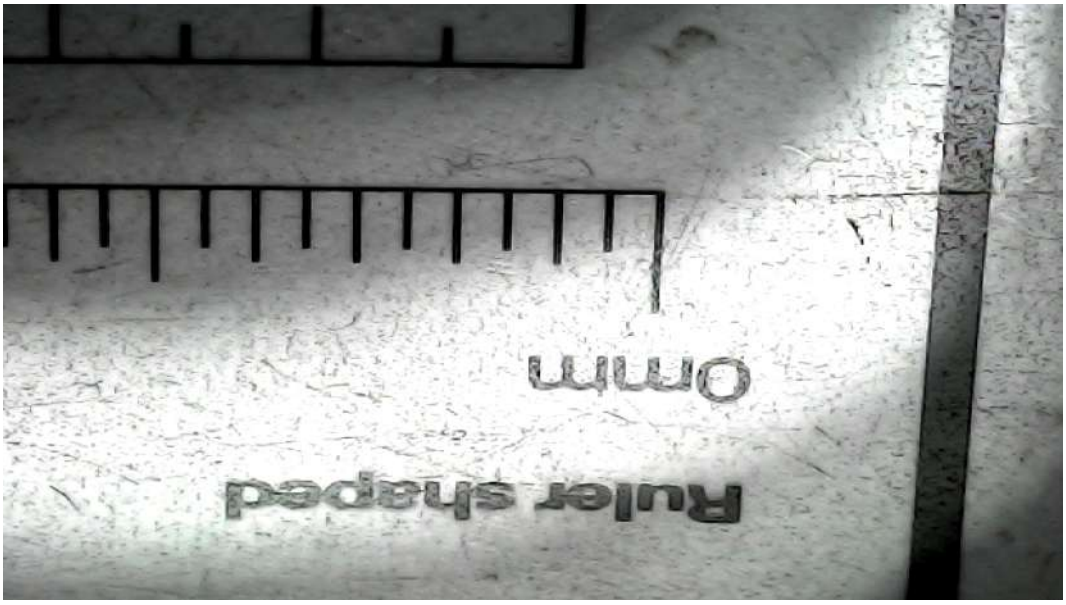

Figure A.1: Calibration scale for USB camera.

Appendix B

Individual tables for the areas under the curves

B.1 Untreated substrates

Table B.1: Areas under the spectra for the scratched and untreated substrates.

Grit	Trial	Area under the curve
1000	1	26946.29893
	2	27065.49798
	3	22371.37661
	4	23617.40642
	5	29515.12940
1500	1	34064.64726
	2	47474.71441
	3	23348.44086
	4	42855.96192
	5	42664.89812
2000	1	24016.06560
	2	23489.36972
	3	26296.73891
	4	18762.32974
	5	21273.16988

B.2 3-second treatments

Table B.2: Areas under the spectra for the substrates treated for 3 seconds.

Grit	Trial	Area under the curve
1000	1	56183.73109
	2	57988.65817
	3	55339.32954
	4	57288.80222
	5	57785.35527
1500	1	47117.39579
	2	52873.29511
	3	56700.58855
	4	57820.05419
	5	55874.30460
2000	1	54568.60464
	2	58311.58275
	3	55956.33672
	4	59503.06155
	5	58986.92213

B.3 5-second treatments

Table B.3: Areas under the spectra for the substrates treated for 5 seconds.

Grit	Trial	Area under the curve
1000	1	47951.67285
	2	45201.71452
	3	42490.06535
	4	36365.86606
	5	45779.77535
1500	1	54599.88101
	2	52832.72175
	3	48995.41216
	4	56816.82841
	5	57473.69924
2000	1	60241.81807
	2	49961.79865
	3	56640.81007
	4	53069.20846
	5	59389.22438

B.4 7-second treatments

Table B.4: Areas under the spectra for the substrates treated for 7 seconds.

Grit	Trial	Area under the curve
1000	1	53556.42935
	2	43102.35811
	3	49812.51085
	4	47008.25513
	5	43638.02508
1500	1	51818.69691
	2	57684.31554
	3	49527.72992
	4	45428.93022
	5	45846.89599
2000	1	47967.21469
	2	56140.59692
	3	46626.71403
	4	57892.62561
	5	46833.84114

B.5 9-second treatments

Table B.5: Areas under the spectra for the substrates treated for 9 seconds.

Grit	Trial	Area under the curve
1000	1	40240.24925
	2	49692.99698
	3	47207.33663
	4	41101.25881
	5	34613.05369
1500	1	48039.80867
	2	46056.41827
	3	50817.26427
	4	46546.80709
	5	46924.43946
2000	1	51079.94657
	2	49536.20844
	3	44385.04201
	4	43897.79142
	5	48354.96931